Design and analysis of synthetic carbon fixation pathways based on novel enzymatic reactions

Vittorio Rainaldi[1,2], Sarah, D'Adamo[2], Nico J. Claassens[1]

[1]Laboratory of Microbiology, Wageningen University, Stippeneng 4, 6708 WE, Wageningen, the Netherlands
[2]Bioprocess Engineering, Wageningen University, Droevendaalsesteeg 1, 6708 PB, Wageningen, the Netherlands

Corresponding authors: NJC nico.claassens@wur.nl and VR vittorio.rainaldi@wur.nl

Abstract

Biological carbon fixation is currently limited to seven naturally occurring pathways, each with its own limitations and constraints. In recent years, computational analyses of known biochemical reaction networks have identified dozens of theoretical carbon fixation pathways, some of which may have the potential to outperform their natural counterparts. This mix and match approach, however, cannot account for those reactions that have not been reported to occur in nature, which heavily limits the possible solution space. Here, we use a bioretrosynthetic approach coupled with expert biochemical knowledge to identify eight novel pathways that leverage enzyme promiscuity and the latent biochemical reaction space. We analyze the thermodynamic, stoichiometric, and kinetic parameters of these pathways and compare them to the ubiquitous Calvin-Benson-Bassham cycle and previously proposed synthetic CO_2 fixation cycles, highlighting advantages and disadvantages. This work highlights the need for enzyme engineering and design in the quest for efficient biological carbon fixation.

Introduction

The Calvin-Benson-Bassham (CBB) cycle is responsible for over 99% of net primary productivity on earth[1]. Despite its dominance, it is a relatively inefficient pathway, requiring a high energy investment in terms of ATP to fix carbon. Furthermore, its key enzyme, rubisco, is rather slow when compared to other naturally occurring carboxylases and it presents a detrimental side activity with oxygen[2,3], which results in

additional energy costs while still leading to partial loss of carbon in a process called photorespiration[4].

Many synthetic carbon fixation pathways have been designed so far by using a mix and match approach that combines enzymes from disparate sources with fast and efficient carboxylases to generate theoretical cycles that have not been described in nature[5–7]. Nevertheless, a recent quantitative analysis of natural and synthetic carbon fixation pathways by L□we and Kremling showed that most pathways are in fact inferior to the CBB cycle or only marginally more efficient[7], likely making the massive engineering efforts required to implement them unjustified.

Almost all of the current synthetic pathway designs, however, are limited by the fact that they only use known enzymatic activities from databases such as KEGG, which vastly limits the possible solution space. Erb, Jones, and Bar-Even have previously put forward a proposal for categorizing pathways based on five levels, with naturally occurring pathways in level one, and synthetic pathways based on new-to-nature enzyme mechanisms in level five[8]. Despite recent progress, designing enzymes with novel mechanisms remains highly challenging[9,10]. For this reason, we focused on level four pathways, namely those that are based on unreported promiscuous enzyme activities and reactions from the latent biochemical space. In this study, we use a combination of bioretrosynthesis and expert biochemical knowledge to generate novel pathway designs and analyze their thermodynamic[11], stoichiometric[12], and kinetic[13] parameters, comparing them to the CBB cycle and highlighting advantages and disadvantages. All these pathways require engineering of at least one enzyme to change its substrate or cofactor specificity or other relevant parameters such as oxygen tolerance. Oxygen tolerance is particularly important in the context of engineering CO_2 fixation in plants and algae, since these organisms produce oxygen as part of photosynthesis, which would lead to the rapid inactivation of oxygen-sensitive enzymes. However, oxygen tolerance is also important in hydrogen-based microbial bioproduction from CO_2, as CO_2 fixation and bioproduction pathways require ATP, which is generated from O_2-dependent respiration.

Overall, this paper provides a novel approach to pathway design and highlights the need for enzyme engineering to achieve efficient carbon fixation, while offering suggestions regarding possible starting points to engineer the proposed pathways.

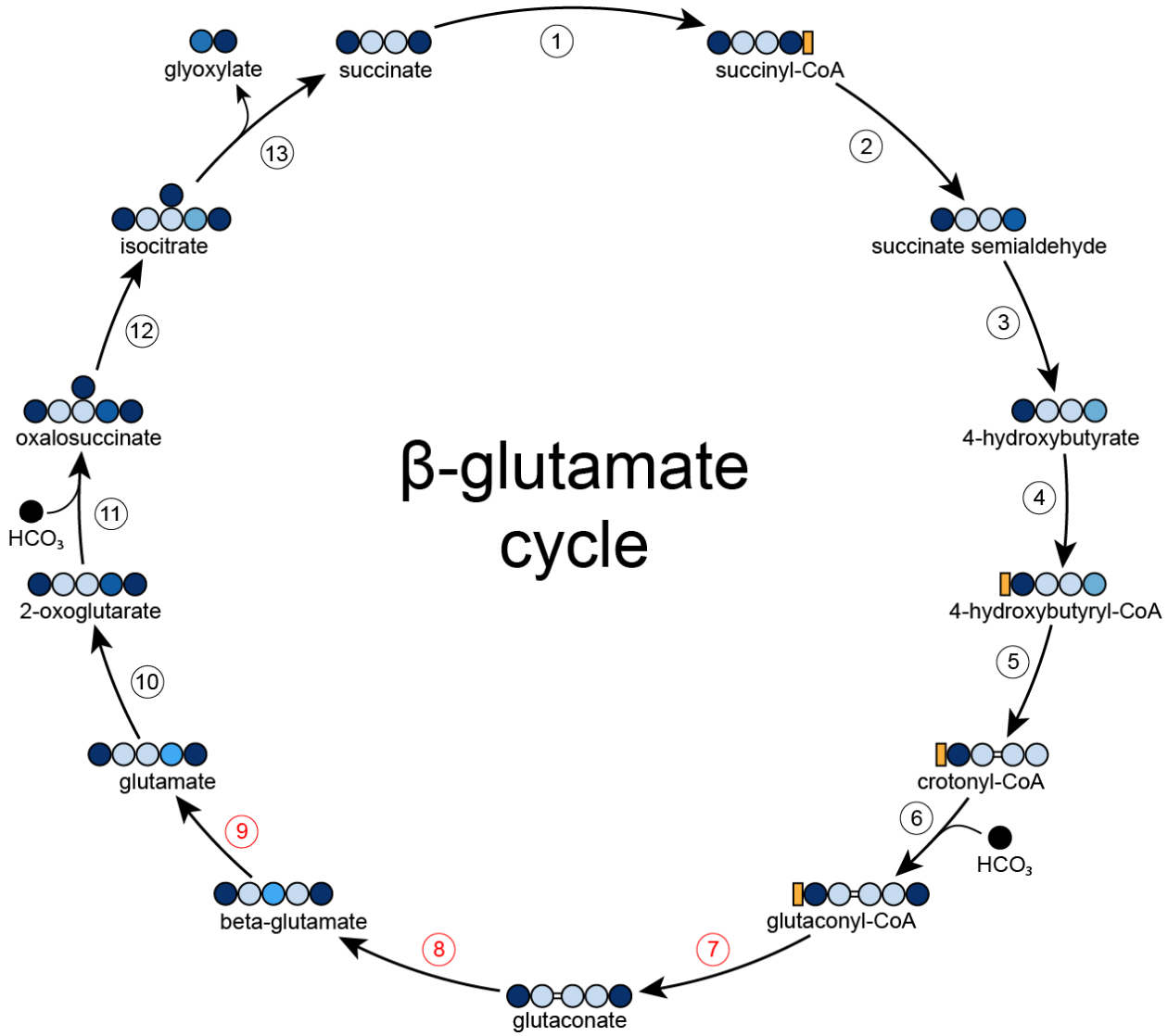

Figure 1: The β-glutamate cycle. 1, succinyl-CoA synthetase; 2, succinyl-CoA reductase; 3, succinate semialdehyde dehydrogenase; 4, 4-hydroxybutyrate CoA transferase; 5, 4-hydroxybutyryl-CoA dehydratase; 6, crotonyl-CoA carboxylase; 7, glutaconate CoA transferase; 8, glutaconate ammonia lyase; 9, glutamate 2,3-aminomutase; 10, glutamate dehydrogenase; 11, 2-oxoglutarate carboxylase; 12, isocitrate dehydrogenase; 13, isocitrate lyase. In this figure and following ones the enzymes marked in red have never been reported in the literature. Bioprospecting or engineering efforts will likely be required to establish their activities.

Results

The β-glutamate cycle

We recently proposed and showed partial in vivo implementation of a new family of carbon fixation pathways called the reductive methylaspartate cycles using the standard mix and match approach[14]. While these cycles are promising, they suffer from two main issues. First, the enzyme crotonyl-CoA carboxylase/reductase (CCR) is relatively inefficient because the NADPH invested for its reductive carboxylation activity is later only partially recovered in the form of a reduced quinone, leading to a loss of energy. Secondly, these cycles require vitamin B_{12} as a cofactor for two enzymatic reactions. Vitamin B_{12} is a highly complex cofactor which cannot be synthesized by most organisms, importantly including all higher plants and many algae[15], thus limiting the applicability of pathways containing B_{12}-dependent enzymes mostly to bacteria.

To overcome both of these issues, we designed a variant of the rMASP cycles that we name the β-glutamate cycle based on its characteristic metabolite. According to our computational analysis, the β-glutamate cycle shows favorable parameters when compared to the CBB, including higher MDF, higher theoretical biomass yield, and comparable pathway activity. These advantages increase in ambient CO_2 environments, with a 40% increase in yield at 20% rubisco oxygenation (Table S1).

The β-glutamate cycle does not use CCR but instead depends on the promiscuous activity of methylcrotonyl-CoA gamma carboxylase (MCC)[16,17], which we will refer to as crotonyl-CoA gamma carboxylase (CCC). This biotin-dependent carboxylase is involved in leucine degradation across diverse phyla including bacteria[18,19] and humans. Its promiscuous side activity on the slightly smaller crotonyl-CoA has been reported in the literature with about 90% of the reaction rate when compared to the native substrate. Since the carboxylation happens in gamma, as opposed to alpha, it produces glutaconyl-CoA instead of ethylmalonyl-CoA, thus obviating the need for a B_{12} dependent mutase to “straighten” the carbon skeleton.

The cycle proceeds with the removal of the CoA from glutaconyl-CoA via a CoA transferase or CoA ligase to yield glutaconate, which is further aminated to 3-aminoglutarate, also known as β-glutamate, which gives its name to the cycle. This amination reaction could be promiscuously performed by aspartate/methylaspartate ammonia lyase[20], though most likely it would require engineering to expand the substrate binding pocket to accommodate one extra carbon. An alternative to this route could be the direct amination of glutaconyl-CoA, for example by a promiscuous β-alanyl-CoA ammonia lyase, an enzyme found in anaerobic bacteria and used for β-alanine fermentation[21]. The resulting beta-glutamyl-CoA would once again require a CoA transferase or CoA ligase to remove the CoA and yield β-glutamate.

At this point, β-glutamate must undergo isomerization to produce glutamate. This reaction is catalyzed by the naturally occurring enzyme glutamate 2,3-aminomutase[22], which is present in bacteria and archaea, respectively for glutamate fermentation and

for the production of beta-glutamate as an osmolyte[23]. This reaction, however, is highly challenging, requiring a radical mechanism based on S-adenosyl-methionine (SAM), making the enzyme oxygen-sensitive. Nevertheless, there are oxygen-tolerant variants reported to catalyze the same reaction aerobically, though using lysine as a substrate as opposed to glutamate[24–26]. Not much is known about this enzyme class, so it is difficult to know whether it would be easier to engineer oxygen-tolerance in a glutamate aminomutase or change substrate specificity in a lysine aminomutase. It must be noted, however, that while there are many examples of oxygen-tolerant radical SAM enzymes[27,28], e.g. *bioB* and *lipA* from *E. coli*, there seems to be a tradeoff between activity and oxygen tolerance, with oxygen-sensitive variants showing higher activity. For this reason, it may not be possible to obtain an oxygen-tolerant aminomutase with comparable kinetic parameters to oxygen-sensitive isoforms.

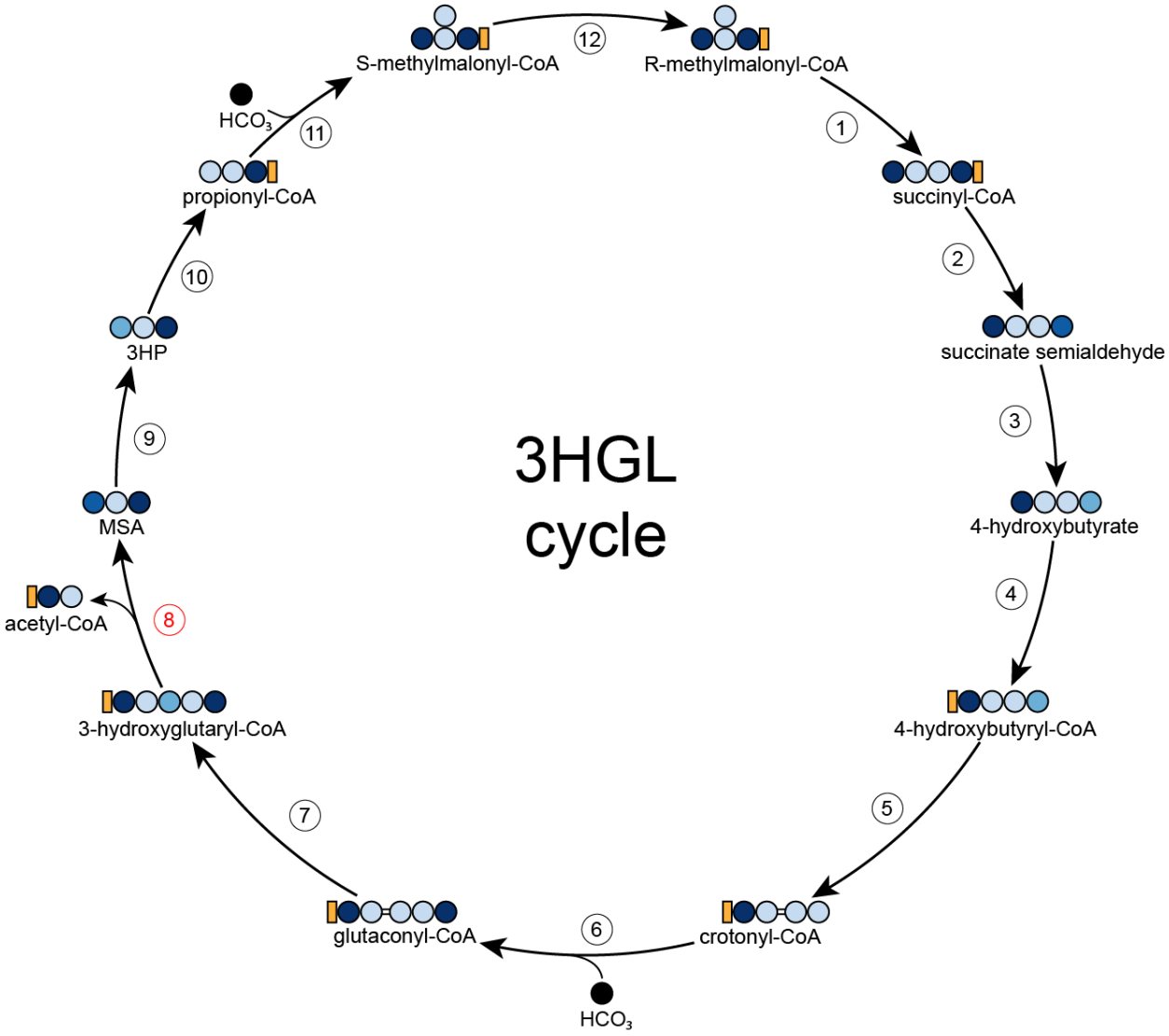

Figure 2: The 3-hydroxyglutaryl-CoA lyase cycle. 1, methylmalonyl-CoA mutase; 2-6 are as in figure 1; 7, glutaconyl-CoA hydratase; 8, 3-hydroxyglutaryl-CoA lyase; 9, malonate semialdehyde reductase; 10, propionyl-CoA synthase; 11, propionyl-CoA carboxylase; 12, methylmalonyl-CoA epimerase.

The 3-hydroxyglutaryl-CoA lyase (3HGL) cycle

In the leucine degradation pathway, the intermediate methylglutaconyl-CoA, product of methylcrotonyl-CoA gamma carboxylase (MCC), undergoes hydration to 3-hydroxy-3-methylglutaconyl-CoA and is subsequently split to acetoacetate and acetyl-CoA. We reasoned that the product of CCC, glutaconyl-CoA, can also undergo hydration rather than amination, yielding 3-hydroxyglutaryl-CoA. This promiscuous reaction is indeed reported to occur efficiently[29]. This metabolite could then be split by 3HMG-CoA lyase to acetyl-CoA and malonate semialdehyde, with the latter being reduced to propionyl-CoA and subsequently carboxylated. The resulting succinyl-CoA can then be reduced to crotonyl-CoA to restart the cycle. More pathways based on CCC and glutaconyl-CoA hydration have previously been reported[5,30], however the authors describe a hydration in C2 rather than C3, which produces 2-hydroxyglutaryl-CoA. Unfortunately, the enzyme that catalyzes this reaction is based on a ketyl radical mechanism and hence extremely oxygen sensitive[31,32]. To the best of our knowledge there has never been a report of ketyl radical enzymes operating in aerobic conditions, making these proposed routes infeasible for aerobic implementation, while their anaerobic implementation would require an external electron acceptor, making the pathways biotechnologically not relevant. The 3HGL cycle, on the other hand, does not use any oxygen-sensitive enzymes, since hydration in C3 occurs easily due to the differences in the pKa between the C2 protons and the C3 protons[33].

This pathway is comparable to the CBB cycle in terms of rate of CO_2 fixation and yield at high CO_2 concentration and it is predicted to have about 27% higher yield at ambient CO_2, with roughly double the activity (Figure 9). Moreover, the addition of acetyl-CoA carboxylase and malonyl-CoA reductase makes the cycle autocatalytic, much like the CBB cycle and reverse tricarboxylic acid (rTCA) cycle. Autocatalytic cycles are expected to be more stable and resilient to metabolic perturbations[34], potentially simplifying engineering efforts. Nevertheless, the strict B_{12} requirement for methylmalonyl-CoA mutase limits its application to bacteria and some algae[15].

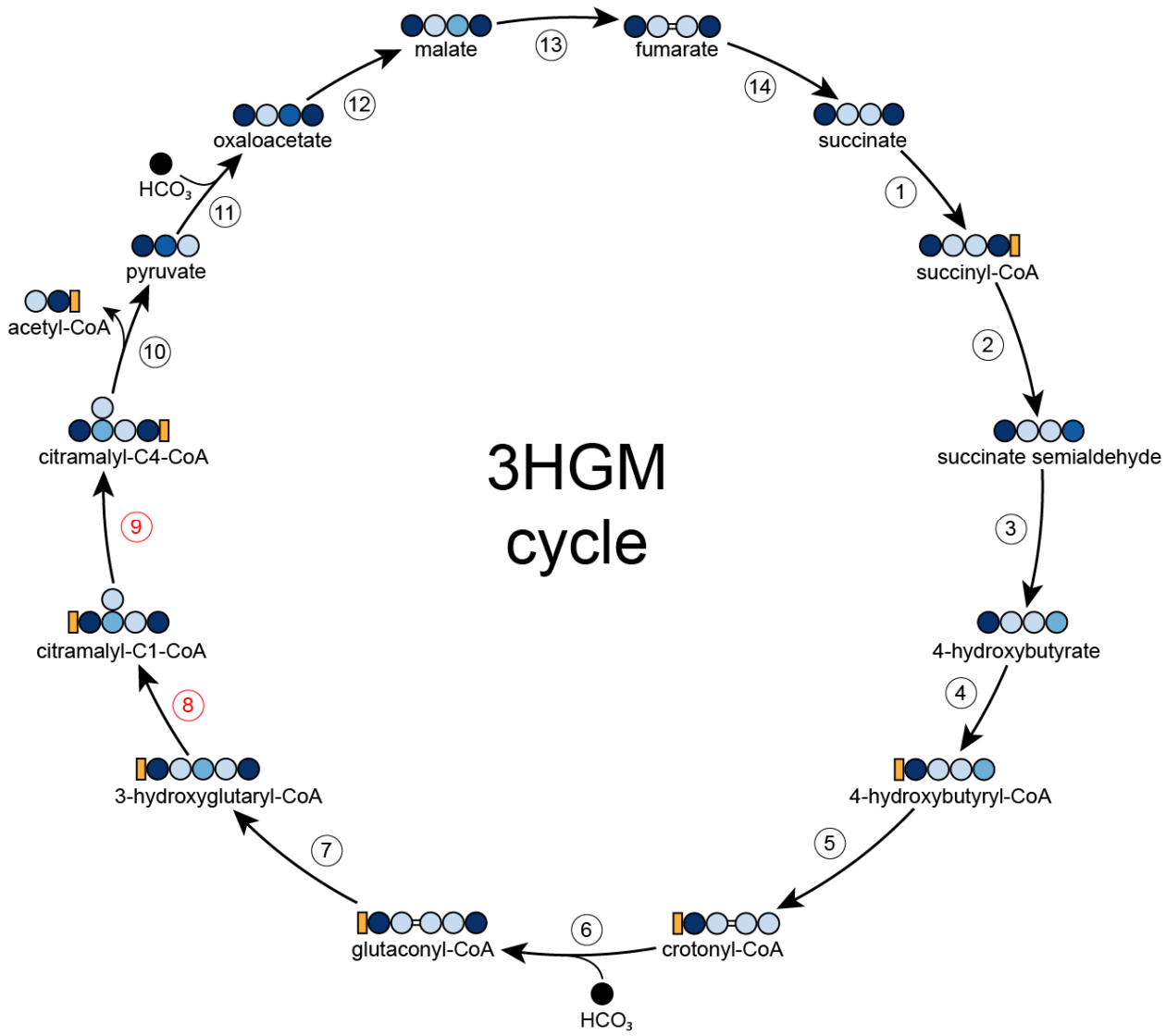

Figure 3: The 3-hydroxyglutaryl-CoA mutase cycle. 1-6 are as in figure 1; 7, glutaconyl-CoA hydratase; 8, 3-hydroxyglutaryl-CoA mutase; 9, citramalyl-CoA transferase; 10, citramalyl-CoA lyase; 11, pyruvate carboxylase; 12, malate dehydrogenase; 13, fumarase; 14, fumarate reductase.

The 3-hydroxyglutaryl-CoA mutase (3HGM) cycle

Alternatively, 3-hydroxyglutaryl-CoA could be isomerized in a similar reaction to the naturally occurring interconversion of 3-hydroxybutyryl-CoA and 2-hydroxyisobutyryl-CoA[35,36], catalyzed by a B_{12}-dependent mutase. It should be noted, however, that the resulting molecule, namely citramalyl-CoA, would carry the CoA on C1 rather than C4, thus requiring a specialized enzyme to swap the CoA, similarly to mesaconyl-CoA transferase[37]. This is necessary because the subsequent citramalyl-CoA lyase reaction is only possible if the CoA is in C4. This same enzyme was recently engineered to

accept 3-hydroxypropionyl-CoA and catalyze its interconversion to lactyl-CoA[38] as part of the previously proposed MOG-LCM cycle[5], which we included in our comparative computational analysis along with the MOG-BAAM cycle from the same paper (Figure 9). This engineering effort produced an enzyme with a poor k_{cat} of 0.03, which is around an order of magnitude lower than the activity on its original substrate. Even this native activity is rather low, and it is unclear whether it can be improved. A computational analysis of the promiscuous activity of B_{12}-dependent glutamate mutase on the alternative substrate 2-hydroxyglutarate (yielding threo-methylmalate) identified a thermodynamic bottleneck in the reaction due to the formation of a glycolyl radical instead of the usual glycyl radical which is formed in the glutamate mutase reaction. The presence of a hydroxyl group in the glycolyl radical is thought to destabilize the radical leading to an increase in activation energy and a proportional decrease in k_{cat} of about two orders of magnitude (5 s^{-1} to 0.05 s^{-1})[39]. It is currently unclear whether this issue can be solved and if it is related to glutamate mutase or general to all B_{12}-dependent mutases. More research will be needed to improve our understanding of the chemistry catalyzed by this complex cofactor.

The α-ketobutyrate carboxylase (ABC) cycles

While pathways based on crotonyl-CoA carboxylation use either the condensation of two acetyl-CoA molecules or the reduction of succinyl-CoA, a different strategy can be envisioned based on the threonine biosynthesis pathway. We recently reported the in vivo implementation of the Serine Threonine Cycle (STC) for full formatotrophic growth

in *E.*

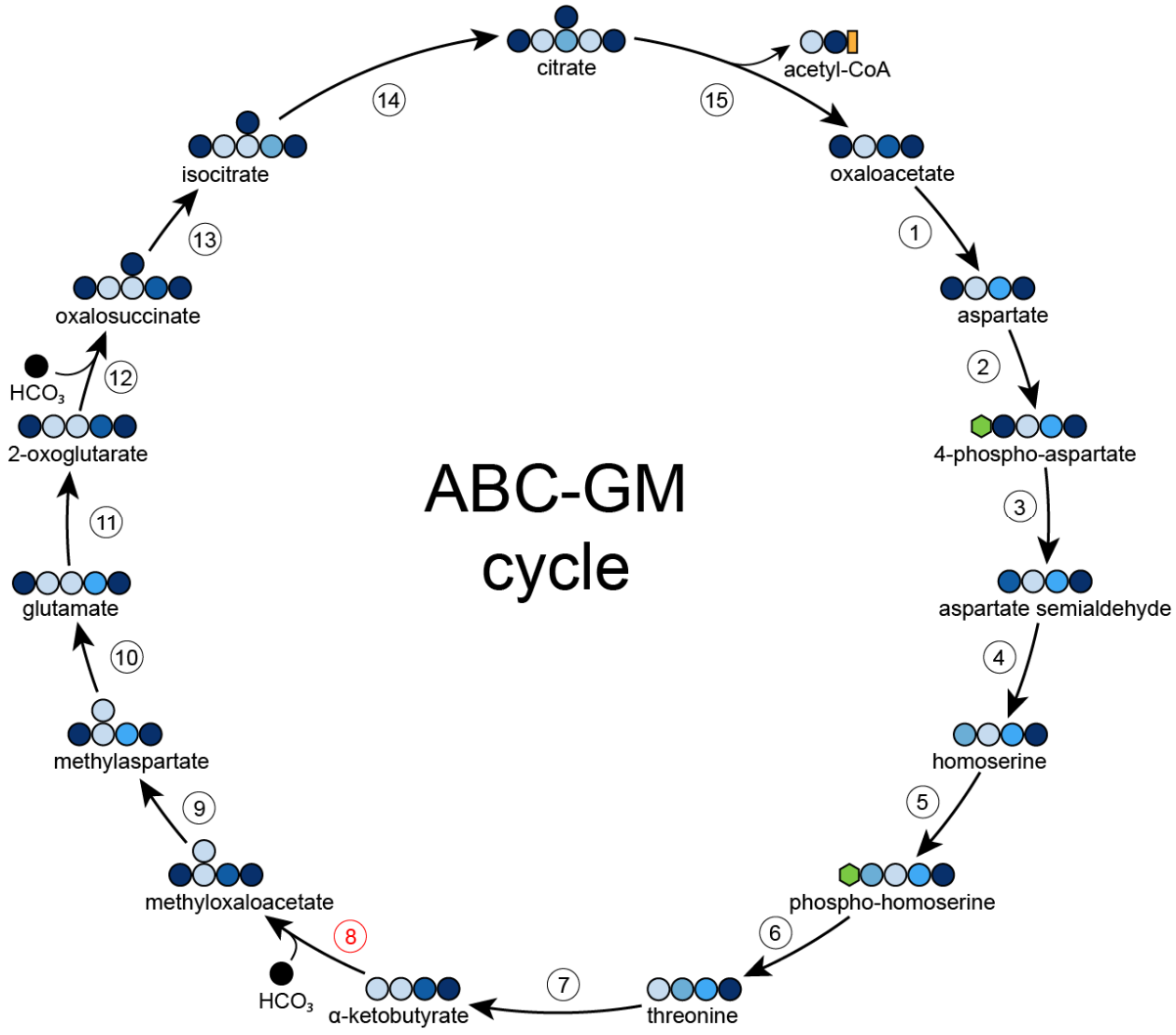

Figure 4: The *α*-ketobutyrate carboxylase-glutamate mutase cycle. 1, aspartate aminotransferase; 2, aspartate kinase; 3, aspartate semialdehyde dehydrogenase; 4, homoserine dehydrogenase; 5, homoserine kinase; 6, threonine synthase; 7, threonine deaminase; 8, *α*-ketobutyrate carboxylase; 9, methylaspartate aminotransferase; 10, glutamate mutase; 11, glutamate dehydrogenase; 12, 2-oxoglutarate carboxylase; 13, oxalosuccinate reductase; 14, aconitase; 15, ATP citrate lyase

coli[40]. The STC relies on the condensation of glycine derived from threonine cleavage with externally supplied formate and an additional carboxylation reaction based on pyruvate carboxylase to regenerate the four-carbon molecule aspartate, which is the precursor for threonine. We reasoned that threonine could instead undergo deamination to produce α-ketobutyrate, which is an α-keto acid highly similar to pyruvate and thus amenable to carboxylation via an engineered pyruvate carboxylase. While we could find

no reports of a biotin-dependent α-ketobutyrate carboxylase in the literature, there is at least one study showing partial promiscuous activity of pyruvate carboxylase on α-ketobutyrate[41]. This limited activity could be used as the basis for mutagenesis or rational engineering in an approach similar to the one used to change the substrate specificity of propionyl-CoA carboxylase to glycolyl-CoA[42].

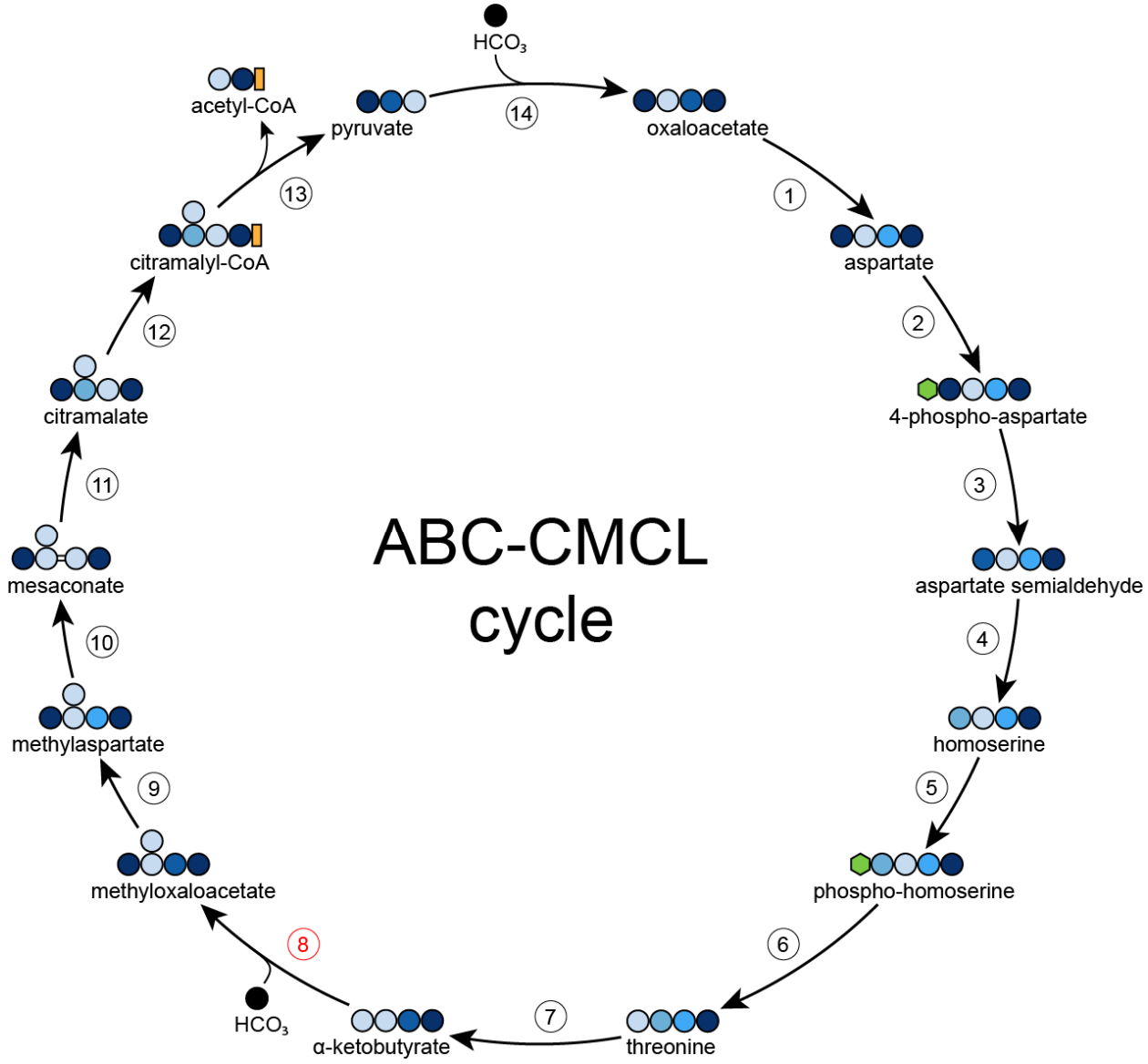

Figure 5: The *α*-ketobutyrate carboxylase-ciramalyl-CoA lyase cycle. 1-9 are as in figure 4. 10, methylaspartate ammonia lyase; 11, mesaconase; 12, citramalate CoA transferase; 13, citramalyl-CoA lyase; 14, pyruvate carboxylase.

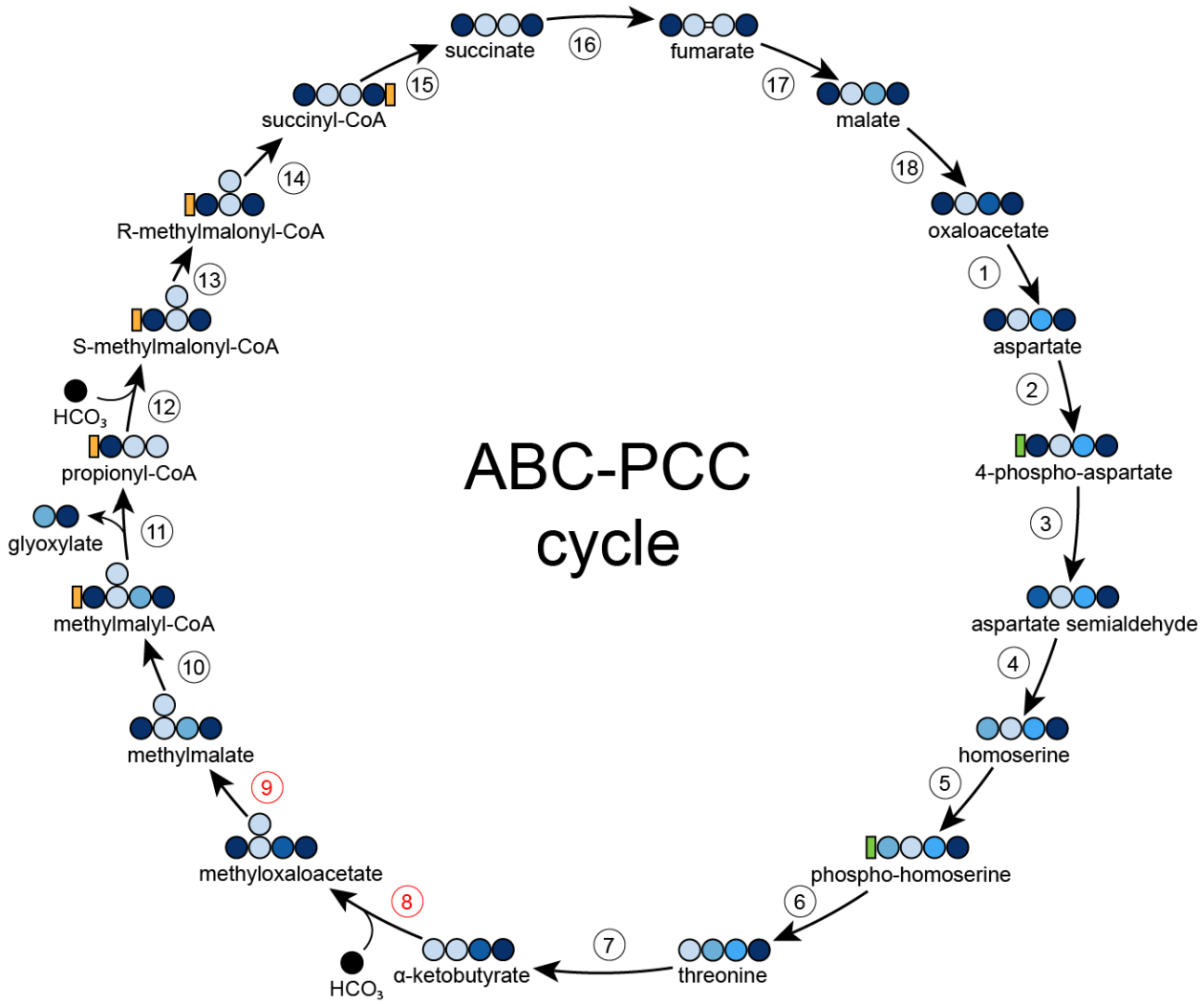

Figure 6: The *α*-ketobutyrate carboxylase-propionyl-CoA carboxylase cycle. 1-8 are as in figures 4 and 5. 9, methylmalate dehydrogenase, 10, methylmalate-CoA transferase; 11, methylmalyl-CoA lyase; 12, propionyl-CoA carboxylase; 13, methylmalonyl-CoA epimerase; 14, methylmalonyl-CoA mutase; 15, succinyl-CoA synthetase; 16, succinate dehydrogenase; 17, fumarase; 18, malate dehydrogenase.

While pyruvate carboxylation produces oxaloacetate, α-ketobutyrate carboxylation would produce 3-methyloxaloacetate (also known as 2-methyl-3-oxosuccinate or oxalopropionate). This compound can undergo reductive amination or transamination to methylaspartate[43], reduction to 3-methylmalate (erythro or threo), or condensation with acetyl-CoA to methylcitrate, though we did not investigate the latter option further. In the first case, methylaspartate can be isomerized to glutamate via a B_{12}-dependent glutamate mutase (GM) and then proceed via the same steps as the previously described rMASP cycles[14]. This variant, which we name ABC-GM cycle, compares favorably to the CBB at ambient CO_2 in terms of biomass yield, though its strict

requirement for B_{12} limits its applicability to microorganisms. To bypass this need, we propose another variant where methylaspartate is deaminated to mesaconate and hydrated to citramalate, which is then activated to citramalyl-CoA and split to pyruvate and acetyl-CoA via a citramalyl-CoA lyase (CMCL). This variant, called ABC-CMCL cycle is slightly less efficient in terms of biomass yield but has a higher predicted pathway activity. A third option could use of the promiscuous activity of malate dehydrogenase (MDH) for the reduction of methyloxaloacetate to erythro-methylmalate, which can further be activated to a CoA ester and split to propionyl-CoA and glyoxylate, however this variant known as ABC-MDH, also requires B_{12} for the isomerization of methylmalonyl-CoA following the carboxylation of propionyl-CoA. Notably, the ABC cycles only require one enzyme to be engineered, and their overlap with the STC shows that they could be engineered relatively easily by applying some of the lessons learned during the STC engineering and evolution[40]. Nevertheless, our theoretical analysis shows that threonine biosynthesis may be limiting the overall activity of the pathway, especially through the bottleneck enzyme homoserine dehydrogenase. It is unclear whether faster variants of this enzyme can be found or engineered, and if the thermodynamic constraints of this biosynthetic route can be overcome, e.g. by optimizing enzymes and/or metabolite concentration. More research will be needed to ascertain whether this theoretical prediction will be verified experimentally.

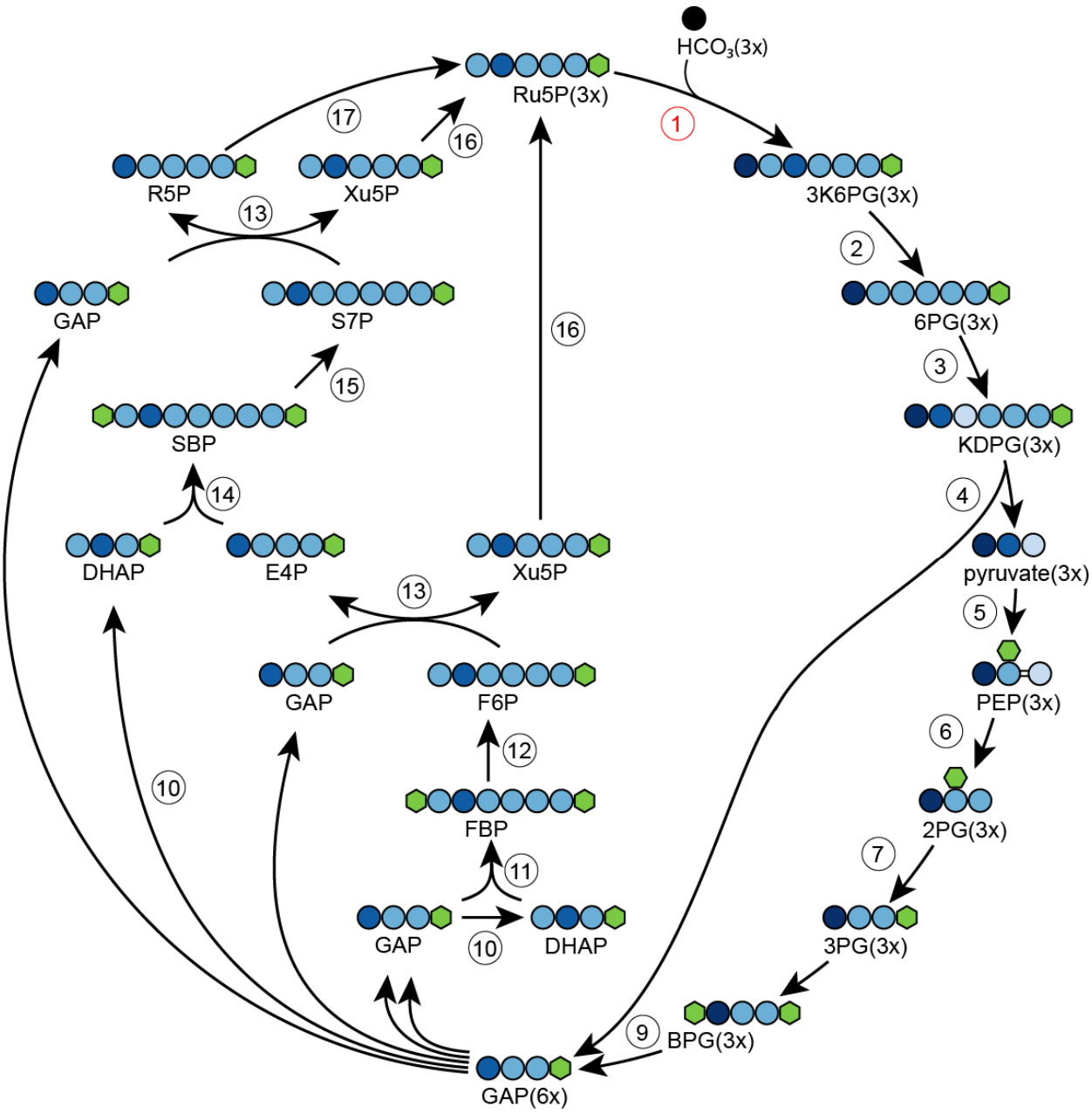

Figure 7: The Ribulose-5-phosphate carboxylase-Entner-Doudoroff (RED) cycle. 2PG, 2-phosphoglycerate; 3K6PG, 3-keto-6-phosphogluconate; 3PG, 3-phosphoglycerate; 6PG, 6-phosphogluconate; BPG, 1,3-bisphosphoglycerate; DHAP, dihydroxyacetone phosphate; E4P, erythrose-4-phosphate; F6P, fructose-6-phosphate; FBP, fructose-1,6-bisphosphate; GAP, glyceraldehyde-3-phosphate; KDPG, 2-keto-3-deoxy-phosphogluconate, PEP, phosphoenolpyruvate; R5P, ribose-5-phosphate; Ru5P, ribulose-5-phosphate; S7P, sedoheptulose-7-phosphate; SBP, sedoheptulose-1,7-bisphosphate; Xu5P, xylulose-5-phosphate; 1, ribulose-5-phosphate carboxylase; 2, 6-phosphogluconate dehydrogenase; 3, Entner-Doudoroff dehydratase; 4, Entner-Doudoroff aldolase; 5, PEP synthetase; 6, enolase; 7, phosphoglycerate mutase, 8,

phosphoglycerate kinase; 9, glyceraldehyde-3-phosphate dehydrogenase; 10, triose phosphate isomerase; 11, fructose bisphosphate aldolase; 12, fructose bisphosphatase; 13, transketolase; 14, sedoheptulose bisphosphate aldolase; 15, sedoheptulose bisphosphatase; 16, ribulose-5-phosphate epimerase; 17, ribulose-5-phosphate isomerase

The Ribulose-5-phosphate carboxylase-Entner-Doudoroff (RED) cycle

While all the cycles presented so far have some advantages over the CBB, it should be noted that that they are all based on completely different architectures, thus requiring extensive engineering efforts to establish in those organisms, including algae and plants, that already use the CBB cycle. For this reason, we set out to establish a carbon fixation cycle that is similar in architecture to the CBB but presents more favorable characteristics in terms of biomass yield and pathway kinetic. The GND-Entner-Doudoroff (GED) cycle has been previously proposed as a promising alternative to the CBB based on natural enzymes[44], however it is severely limited by the low activity and affinity for CO_2 of its signature enzyme, 6-phosphogluconate dehydrogenase (GND). This enzyme normally catalyzes the oxidative decarboxylation of 6-phosphogluconate, coupling the highly favorable decarboxylation reaction to the unfavorable generation of NADPH. This same mechanism can be found in at least two other central metabolic enzymes, namely the malic enzyme, which produces pyruvate and NADPH from malate, and isocitrate dehydrogenase, which produces α-ketoglutarate and NADPH from isocitrate.

Notably, in both of these cases there is a biotin-dependent carboxylase to overcome the unfavorable thermodynamics and kinetics of this half-reaction, which is then coupled to a dehydrogenase/reductase. Pyruvate is carboxylated to oxaloacetate which is then reduced to malate, while α-ketoglutarate is carboxylated to oxalosuccinate and then reduced to isocitrate[45–47]. A similar idea could be applied to the product of GND, ribulose-5-phosphate. A biotin-dependent carboxylase acting on this substrate would generate 3-keto-6-phosphogluconate, which would then be reduced to 6-phosphogluconate. For this latter reaction GND itself could be used, provided the residues involved in the decarboxylation half-reaction are inactivated. To the best of our knowledge, there is no reported enzyme taking a similar substrate for the carboxylation reaction, meaning that an extensive engineering campaign will be necessary to change the substrate specificity. This is probably beyond what is achievable with current strategies based on mutagenesis and selection, however it may become possible in the future to apply novel enzyme design approaches to redesign the substrate pocket. The RED cycle is insensitive to the presence of oxygen, does not require CoA or exotic cofactors, it is favorable in terms of efficiency and kinetics at ambient CO_2, and it has a high degree of overlap with the CBB cycle, making it a good candidate for implementation in algae and plants, though it should be noted that these organisms do

not express lower glycolysis enzymes in their chloroplasts, which could increase the engineering complexity.

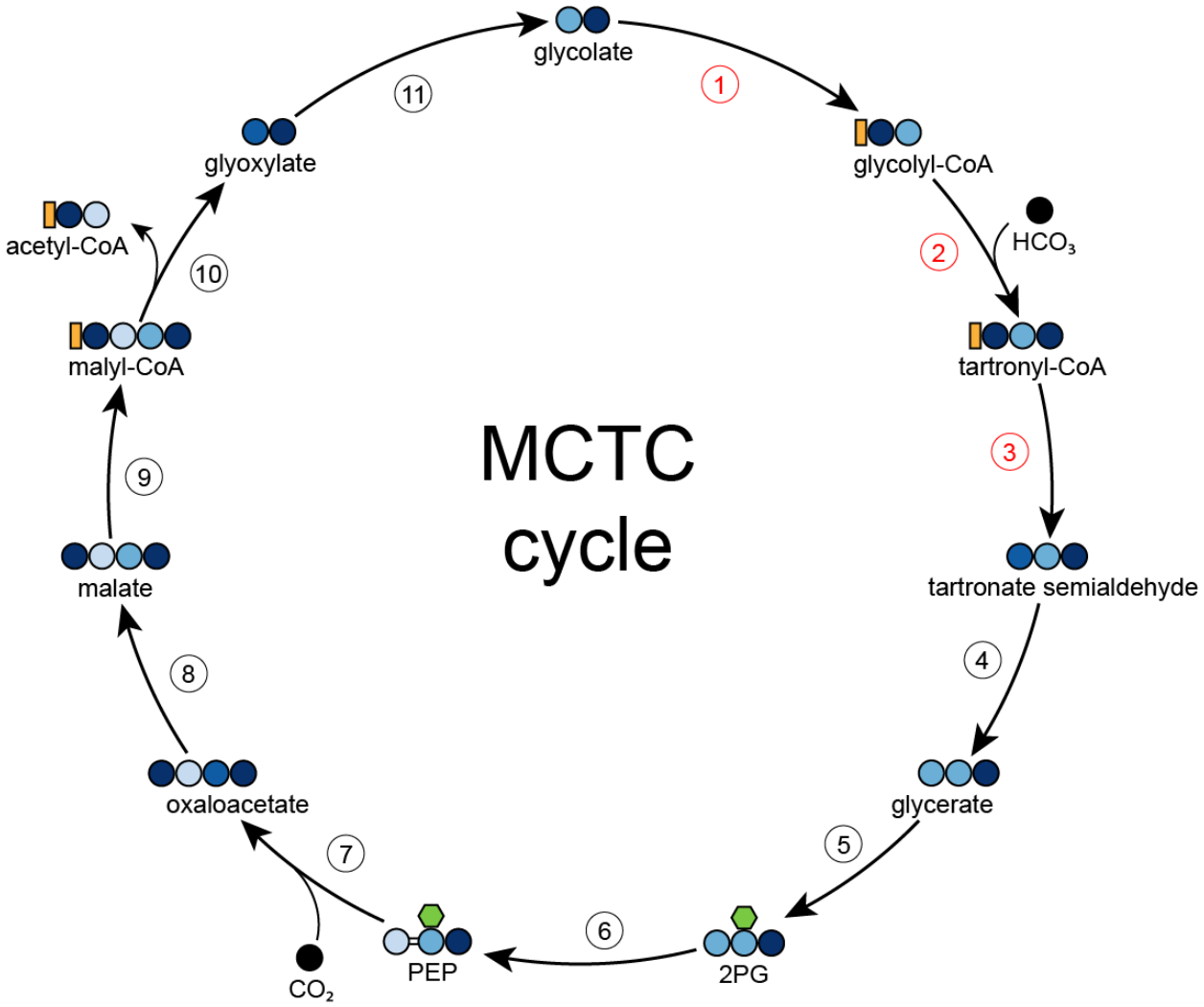

Figure 8: The Malyl-CoA-Tartronyl-CoA (MCTC) cycle. 1, glycolate-CoA ligase; 2, glycolyl-CoA carboxylase; 3, tartronyl-CoA reductase; 4, tartronate semialdehyde reductase; 5, glycerate kinase; 6, enolase; 7, PEP carboxylase; 8, malate dehydrogenase; 9, malate CoA transferase; 10, malyl-CoA lyase; 11, glyoxylate reductase.

The Malyl-CoA-Tartronyl-CoA (MCTC) pathway

Scheffen et al. recently reported engineered a biotin-dependent propionyl-CoA carboxylase to accept the smaller substrate glycolyl-CoA[42]. The resulting enzyme has been named glycolyl-CoA carboxylase (GCC). This carboxylation reaction produces tartronyl-CoA, which is further reduced by an engineered malonyl-CoA reductase to tartronate semialdehyde, which is itself reduced to glycerate, a compound that can

easily be assimilated into central metabolism. The resulting pathway, known as the tartronyl-CoA (TaCo) pathway, was conceived as a photorespiration bypass, taking 2-phosphoglycolate derived from the rubisco oxygenation side reaction and recycling it to 3-phosphoglycerate while not only preventing loss of carbon but fixing carbon instead. While this approach is promising, it is currently hampered by the inefficiency of glycolyl-CoA carboxylase, which hydrolyzes more than 5 ATP per carboxylation reaction, as opposed to 1 ATP for PCC and similar biotin-dependent enzymes. This could be attributed to the difference between propionyl-CoA and glycolyl-CoA as substrates: the latter is not only smaller but contains a hydroxyl group. The presence of a hydroxyl group could destabilize the enolate intermediate required for carboxylation, leading to futile cycles where CO_2 is released into the active site but is unable to react with the substrate. In a subsequent work, the enzyme was further engineered by using a machine-learning guided approach, obtaining improved variants with reduced futile ATP hydrolysis, albeit at the expense of lower overall catalytic activity[48]. Whether this issue can be fully solved remains an open question.

We reasoned that the TaCo pathway could also serve as the basis for a synthetic CO_2 fixation cycle (Figure 8) where the product, glycerate, goes through lower glycolysis and anaplerosis to malate, which is activated to malyl-CoA and split to acetyl-CoA, which is the end product of this cycle, and glyoxylate, which can be reduced to glycolate to restart the cycle. This pathway has the advantage of being relatively compact, requiring only eleven genes for its implementation, all of which have been tested in vitro, potentially making it easier to engineer, especially in less genetically accessible organisms. Assuming an improved GCC can be engineered, we calculated that this cycle is about 20% more efficient than the CBB cycle at ambient CO_2, with comparable pathway activity. We note that while writing this manuscript, this pathway has also been proposed in another work, in which it has been named the LATCH pathway[49].

Coupling the CO_2 reduction (CORE) cycle to formatotrophic pathways

An interesting alternative to CO_2 fixation cycles was recently proposed by Satanowski et al., who theorized a number of oxygen tolerant CO_2 reduction (CORE) cycles and implemented one of them in *E. coli*[50]. The experimentally validated CORE variant relies on the promiscuous activity of a β-keto-acid cleavage enzyme (BKACE) and yields one molecule of formate from one molecule of bicarbonate with the input of one NADPH and 1-3 ATP. While the CORE cycle was originally proposed as a photorespiration bypass, the resulting formate could be fully coupled to growth via a formatotrophic pathway such as the serine cycle. We have modeled the resulting pathway to compare it with our proposed CO_2 fixation cycles (Figure 9). Based on our results, the CORE+Serine cycle shows a comparable yield to the CBB in high CO_2 and a roughly 20% higher yield in ambient CO_2. Assuming the activity of the limiting enzyme, BKACE, can be improved, the CORE+Serine cycle could be a highly relevant alternative to conventional CO_2

fixation cycles, since it is oxygen-tolerant, does not require B_{12}, and mostly relies on reactions that are natively present in plants, or that have been shown to be functional after heterologous expression.

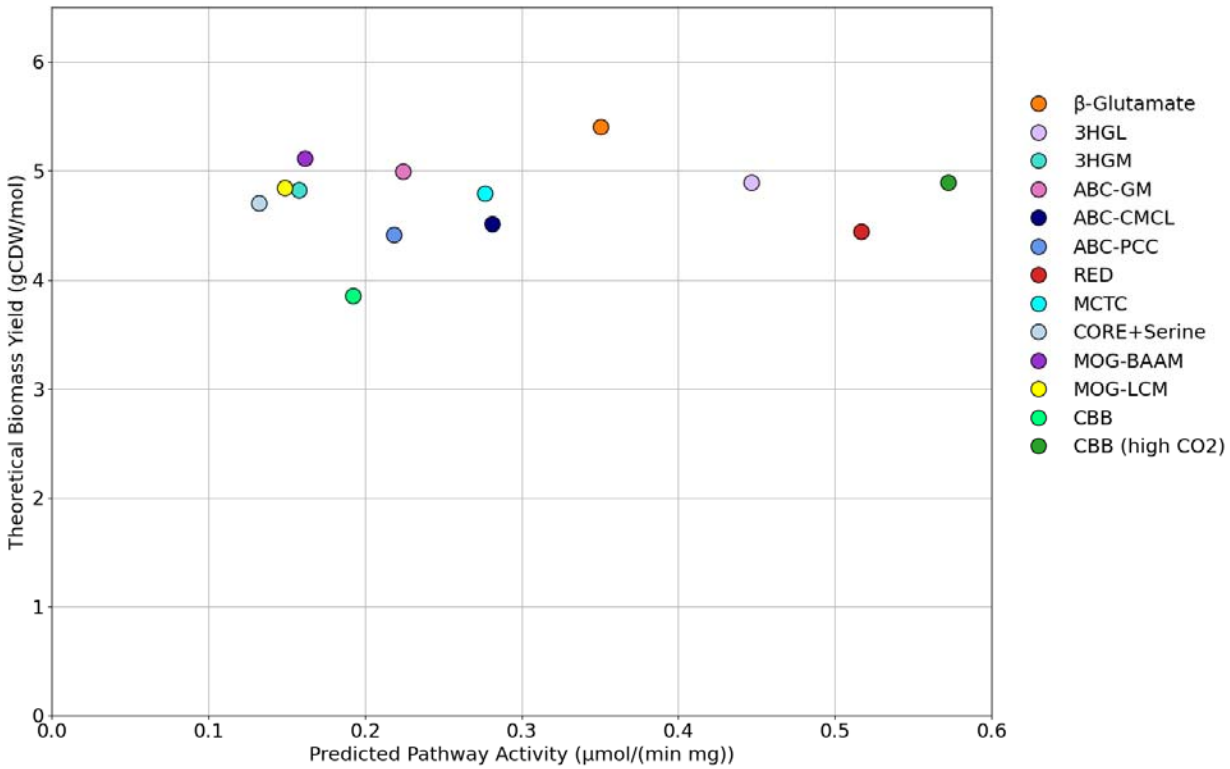

Figure 9: Plot of theoretical biomass yield vs predicted pathway activity for each pathway presented in this paper and previously proposed pathways. This figure includes only pathways that require enzyme engineering for their implementation (other than the CBB cycle). For additional comparisons to previously proposed mix-and-match pathways see figure S1.

Discussion

In this paper, we proposed eight novel carbon fixation pathways based on non-natural enzymatic reactions. We analysed the pathways based on thermodynamic driving force, predicted biomass yield, and predicted pathway activity. This last parameter is computed based on the measured or estimated k_{cat} and K_M values for the enzymes. Unfortunately, the available enzymatic data in databases such as BRENDA is both limited and noisy, since different authors perform enzymatic assays in wildly different conditions in terms of pH, buffers, temperatures, etc. We carefully curated the chosen values, also based on the previous work by Lowe and Kremling, however a relatively large fraction of the enzymes was only measured in single studies, reducing their reliability. Where multiple data points are available, it is not unusual to see a variation of one order of magnitude or more in reported k_{cat} and K_M.

Furthermore, in vitro kinetics measurements, even when performed properly, are based on a purified enzyme in a dilute buffer, which is a completely different scenario compared to the densely packed cytosol of living organisms, where thousands of enzymes and metabolites are present. Recent work has shown k_{cat} measurements in vivo based on different growth conditions and proteomics data[51]. These results show that while many in vitro measurements are also accurate in vivo, there are several outliers even for well characterized enzymes in central metabolism, with a relatively weak correlation R^2 of 0.62. All these problems are compounded when it comes to relatively understudied enzymes, and especially their promiscuous activities. Finally, the kinetic parameters of not yet existing enzymes are obviously impossible to obtain, and we have simply taken representative values for similar enzymes on related substrates.

ECM measurements assume an optimal distribution of metabolites and enzymes, and do not take into account enzyme degradation, allosteric inhibition, competitive inhibition, and regulation. They also do not consider all the enzymes that are necessary for cell maintenance and growth, assuming all flux is going via the pathway of interest to generate the desired product. In practice, all these factors mean that the predicted pathway activity is at best an upper bound for the real pathway activity in a real-life scenario. Taking the CBB into account, measured values for CO_2 fixation rates in exponentially growing bacteria are in the order of 3-9 nmol/min/mg (total) protein[52]. This is a two order of magnitude difference below our computed value of around 0.5 µmol/min/mg (pathway) protein. This discrepancy is partially explained when taking into account the fact that CBB enzymes account for about 10% of total protein [53]. The predicted pathway activity for the CBB, then, is still one order of magnitude above measured values, despite the fact that all of its the enzymes are well-characterized in dozens of studies.

For the other pathways, greater uncertainty is expected due to the limited reliability of the available data. It is unclear whether this uncertainty leads to an overestimate or an underestimate of the total pathway activity, however it is likely that for most of the candidate enzymes, kinetically superior isoforms could be found through a screening process. This points to the fact that pathways other than the CBB may be underestimated in our analysis. Further research will be needed to determine real life (i.e. in vivo) kinetic parameters for several enzymes, leading to better estimates.

Considering all of this, our proposed pathways are especially promising for potential future applications in terms of yield, as they can outcompete the CBB cycle, even at high CO_2, especially the β-glutamate cycle (10% or 40% higher yield than CBB cycle at high and ambient CO_2 respectively), and also the 3HGL, 3HGM, ABC-GM and MOG-BAAM may outperform the CBB cycle slightly at high CO_2 and by >30% in yield at ambient CO_2. However, none of them is predicted so far to outperform the CBB in terms of pathway activity, at least in the high CO_2 scenario. Still, the β-glutamate cycle, 3HGL

and RED cycles are close (having 61%, 70% and 90% of predicted pathway activity of the CBB cycle at high CO_2). Overall, this makes especially the β-glutamate and 3HGL cycles promising to explore, given a potentially attractive yield, and reasonable predicted pathway activity. As discussed above, pathway activity may be further increased based on natural enzyme screening and enzyme engineering and evolution efforts. The β-glutamate cycle especially stands out compared to 3HGL as it does not require B_{12} and could potentially also be implemented in photosynthetic microalgae and plants. However, given its required three new-to-nature activities and relatively large pathway size this would be a tremendous engineering effort already in bacteria, and definitely in microalgae and plants. The RED cycle, on the other hand, could be highly relevant based on its overlap with the CBB and high predicted pathway activity, while the ABC cycle strike a balance between yield, activity, and ease of implementation, since they require only one engineered enzyme and otherwise rely on the naturally occurring and widespread threonine biosynthesis route.

The fact that all pathways are predicted to be slower than the CBB cycle also highlights the fact that carbon fixation cycles are not only limited by carboxylation activity and that Rubisco, despite its relatively slow catalysis and oxygenation side activity, still leads to relatively high pathway activity when considered in its metabolic context[54].

An open question remains for the field: why is the CBB ubiquitous, if stoichiometrically and/or kinetically superior pathways are potentially possible? One possible explanation for this is the high degree of overlap between the CBB cycle and the pentose phosphate pathway, which exists in all living organisms. In fact, only Rubisco and PRK are necessary on top of the standard pentose phosphate pathway genes, as demonstrated by the engineering of *E. coli* to grow autotrophically via the CBB cycle, and it is common in nature for these two genes to be expressed from a plasmid, which can easily be horizontally transferred, thus spreading the CBB cycle across phyla. Furthermore, several essential biomass precursors are formed as part of the cycle, which would make a loss of activity detrimental. At least in the short term, an organism that acquired all the necessary genes to support an alternative carbon fixation cycle pathway would have to support both cycles at the same time, likely with competing if not outright incompatible fluxes and metabolic profiles. The engineering approach to rewiring metabolism uses autotrophies and bypasses to force metabolic rearrangements[55]. This strategy has proven highly reliable in engineering a diverse array of pathways and will likely be just as useful in the future[40,56–59].

Overall, our study expands the solution space for carbon fixation by providing realistic and biochemically feasible avenues for enzymatic transformations based on known enzyme mechanisms and substrate promiscuity. Notably, we identified two potential novel carboxylases that could lead to entirely new pathway architectures once implemented. New carbon fixation pathways with better yield and insensitivity to oxygen

could lead to improved carbon fixation in algae or plants, potentially leading to renewable production of chemicals and increases in crop yields.

Methods

All scripts and input files are available on gitlab (https://git.wur.nl/vittorio.rainaldi/lvl4). All pathways were computationally analyzed using flux balance analysis[60] (FBA) with cobrapy[61] (version 0.29.1) using the *E. coli* iML1515[12] genome scale-metabolic model. The base model was modified to change membrane-bound transhydrogenase (TDH2pp) to translocate one proton rather than two[62]. Anaerobic reactions such as PFL, OBTFL, and POR5 were set to zero. Non-growth associated maintenance (ATPM) was set to zero. Additional modifications were added for each individual pathway. FBA returns a flux value in gCDW/mol substrate. In this case, since CO_2 is freely available in the atmosphere, it was left unconstrained, however an energy source is required to run CO_2 fixation cycle, and this was used as a constraint for all pathways. For this purpose, we added a dummy reaction which produces NADPH, which is the main source of reducing power in photosynthetic organisms such as algae and plants. This results in slightly higher values compared to using NADH as an energy source, since NADH to NADPH conversion requires the translocation of one proton, which amounts to roughly one-third of one ATP[62].

Max-min driving force[11] and enzyme cost[13] were computed with a custom script modified from previous work[44,63] using equilibrator (version 0.6.0). Metabolite concentrations were constrained to the physiologically relevant range between 10 µM and 10 mM. ECM was computed using the following parameters: algorithm ECM, version 3, kcat_source fwd, denominator CM, regularization volume, p_h 7.5, ionic_strength 0.3 molar, p_mg 3, dg_confidence 0.95. Kinetics values were taken from Brenda[64] or previous work[7]. In the case of new-to-nature enzymatic activities, the kinetics were estimated by taking values from similar enzymes. For example, kinetic values for α-ketobutyrate carboxylase are not available, so values for pyruvate carboxylase were used instead. Since this enzyme catalyzes the same reaction on a slightly smaller substrate, it is reasonable to assume that an engineered enzyme could reach similar kinetic properties. The ECM algorithm returns a list of enzyme costs in moles of enzyme per liter based on a total flux through the pathway for 1 mM/s of product formed. These values were multiplied by the molecular weight of the respective enzyme to obtain the enzyme cost in g/l. The sum of all the values is the enzyme cost (EC) for the pathway. To obtain the pathway activity we performed the following calculations:

$$\text{Pathway activity} = \frac{\mu mol}{\min * mg}$$

flux = x $\frac{mM}{s} = 1000x\frac{\mu M}{s} = 60000x\frac{\mu M}{min} = 60000x\ \frac{\mu mol}{\text{min}*L}$

Enzyme Cost (EC) = y $\frac{g}{L} = 1000y\frac{mg}{L}$

Pathway activity = $60000x\ \frac{\mu mol}{\text{min}*L}\left(\frac{1}{1000y}\right)\frac{L}{mg} = 60\frac{x}{y}\frac{\mu mol}{\text{min}*mg}\ =\ 60\frac{flux}{EC}$

References

1. *The Prokaryotes*. (Springer Berlin Heidelberg, Berlin, Heidelberg, 2013). doi:10.1007/978-3-642-30123-0.
2. Prywes, N., Phillips, N. R., Tuck, O. T., Valentin-Alvarado, L. E. & Savage, D. F. Rubisco Function, Evolution, and Engineering. *Annu. Rev. Biochem.* **92**, 385–410 (2023).
3. Tcherkez, G. G. B., Farquhar, G. D. & Andrews, T. J. Despite slow catalysis and confused substrate specificity, all ribulose bisphosphate carboxylases may be nearly perfectly optimized. *Proceedings of the National Academy of Sciences* **103**, 7246–7251 (2006).
4. Claassens, N. J. *et al.* Phosphoglycolate salvage in a chemolithoautotroph using the Calvin cycle. *Proc. Natl. Acad. Sci. U.S.A.* **117**, 22452–22461 (2020).
5. Bar-Even, A., Noor, E., Lewis, N. E. & Milo, R. Design and analysis of synthetic carbon fixation pathways. *Proceedings of the National Academy of Sciences* **107**, 8889–8894 (2010).
6. Schwander, T., Von Borzyskowski, L. S., Burgener, S., Cortina, N. S. & Erb, T. J. A synthetic pathway for the fixation of carbon dioxide in vitro. *Science* **354**, 900–904 (2016).
7. Löwe, H. & Kremling, A. In-Depth Computational Analysis of Natural and Artificial Carbon Fixation Pathways. *BioDesign Research* **2021**, 1–23 (2021).

8. Erb, T. J., Jones, P. R. & Bar-Even, A. Synthetic metabolism: metabolic engineering meets enzyme design. *Current Opinion in Chemical Biology* **37**, 56–62 (2017).
9. Vornholt, T. *et al.* Artificial metalloenzymes. *Nat Rev Methods Primers* **4**, 78 (2024).
10. Zou, Z. *et al.* De novo design and evolution of an artificial metathase for cytoplasmic olefin metathesis. *Nat Catal* 1–12 (2025) doi:10.1038/s41929-025-01436-0.
11. Noor, E. *et al.* Pathway Thermodynamics Highlights Kinetic Obstacles in Central Metabolism. *PLoS Computational Biology* **10**, (2014).
12. Monk, J. M. *et al.* iML1515, a knowledgebase that computes Escherichia coli traits. *Nat Biotechnol* **35**, 904–908 (2017).
13. Noor, E. *et al.* The Protein Cost of Metabolic Fluxes: Prediction from Enzymatic Rate Laws and Cost Minimization. *PLoS Computational Biology* **12**, 1–29 (2016).
14. Rainaldi, V. *et al.* Modular in vivo engineering of the reductive methylaspartate cycles for synthetic CO2 fixation. 2025.11.12.688011 Preprint at https://doi.org/10.1101/2025.11.12.688011 (2025).
15. Croft, M. T., Lawrence, A. D., Raux-Deery, E., Warren, M. J. & Smith, A. G. Algae acquire vitamin B12 through a symbiotic relationship with bacteria. *Nature* **438**, 90–93 (2005).
16. Alban, C., Baldet, P., Axiotis, S. & Douce, R. Purification and Characterization of 3-Methylcrotonyl-Coenzyme A Carboxylase from Higher Plant Mitochondria. *Plant Physiol.* **102**, 957–965 (1993).
17. Huang, C. S., Ge, P., Zhou, Z. H. & Tong, L. An unanticipated architecture of the 750-kDa α6β6 holoenzyme of 3-methylcrotonyl-CoA carboxylase. *Nature* **481**, 219–223 (2012).

18. Chavez-Avilas, M., Díaz-Pérez, A. L., Reyes-de la Cruz, H. & Campos-García, J. The *Pseudomonas aeruginosa liuE* gene encodes the 3-hydroxy-3-methylglutaryl coenzyme A lyase, involved in leucine and acyclic terpene catabolism. *FEMS Microbiology Letters* **296**, 117–123 (2009).
19. Wang, H. *et al.* An essential bifunctional enzyme in *Mycobacterium tuberculosis* for itaconate dissimilation and leucine catabolism. *Proc. Natl. Acad. Sci. U.S.A.* **116**, 15907–15913 (2019).
20. Raj, H. *et al.* Engineering methylaspartate ammonia lyase for the asymmetric synthesis of unnatural amino acids. *Nature Chem* **4**, 478–484 (2012).
21. Herrmann, G. *et al.* Two beta-alanyl-CoA:ammonia lyases in Clostridium propionicum. *The FEBS Journal* **272**, 813–821 (2005).
22. Ruzicka, F. J. & Frey, P. A. Glutamate 2,3-aminomutase: A new member of the radical SAM superfamily of enzymes. *Biochimica et Biophysica Acta (BBA) - Proteins and Proteomics* **1774**, 286–296 (2007).
23. Tunçkanat, T. *et al.* Lysine 2,3-Aminomutase and a Newly Discovered Glutamate 2,3-Aminomutase Produce β-Amino Acids Involved in Salt Tolerance in Methanogenic Archaea. *Biochemistry* **61**, 1077–1090 (2022).
24. Chen, D., Ruzicka, F. J. & Frey, P. A. A novel lysine 2,3-aminomutase encoded by the yodO gene of Bacillus subtilis□: characterization and the observation of organic radical intermediates. 11 (2000).
25. Chen, D., Frey, P. A., Lepore, B. W., Ringe, D. & Ruzicka, F. J. Identification of Structural and Catalytic Classes of Highly Conserved Amino Acid Residues in Lysine 2,3-Aminomutase. *Biochemistry* **45**, 12647–12653 (2006).

26. Behshad, E. *et al.* Enantiomeric Free Radicals and Enzymatic Control of Stereochemistry in a Radical Mechanism: The Case of Lysine 2,3-Aminomutases. *Biochemistry* **45**, 12639–12646 (2006).
27. Sofia, H. J., Chen, G., Hetzler, B. G., Reyes-Spindola, J. F. & Miller, N. E. Radical SAM, a novel protein superfamily linking unresolved steps in familiar biosynthetic pathways with radical mechanisms: functional characterization using new analysis and information visualization methods. *Nucleic Acids Res* **29**, 1097–1106 (2001).
28. Booker, S. J. & Lloyd, C. T. Twenty Years of Radical SAM! The Genesis of the Superfamily. *ACS Bio Med Chem Au* **2**, 538–547 (2022).
29. Mack, M. *et al.* 3-Methylglutaconyl-CoA hydratase from Acinetobacter sp. *Arch Microbiol* **185**, 297–306 (2006).
30. Liu, Y. *et al.* Systematic design and evaluation of artificial CO2 assimilation pathways. *Synthetic and Systems Biotechnology* **10**, 1107–1118 (2025).
31. Kim, J., Hetzel, M., Boiangiu, C. D. & Buckel, W. Dehydration of (*R*)-2-hydroxyacyl-CoA to enoyl-CoA in the fermentation of α-amino acids by anaerobic bacteria. *FEMS Microbiol Rev* **28**, 455–468 (2004).
32. Kim, J., Darley, D. J., Buckel, W. & Pierik, A. J. An allylic ketyl radical intermediate in clostridial amino-acid fermentation. *Nature* **452**, 239–242 (2008).
33. Bahnson, B. J., Anderson, V. E. & Petsko, G. A. Structural Mechanism of Enoyl-CoA Hydratase: Three Atoms from a Single Water Are Added in either an E1cb Stepwise or Concerted Fashion'. *Biochemistry* **41**, 2621–2629 (2002).
34. Hordijk, W. Autocatalytic confusion clarified. *Journal of Theoretical Biology* **435**, 22–28 (2017).

35. Kurteva-Yaneva, N. *et al.* Structural Basis of the Stereospecificity of Bacterial B12-dependent 2-Hydroxyisobutyryl-CoA Mutase. *Journal of Biological Chemistry* **290**, 9727–9737 (2015).
36. Rohwerder, T., Rohde, M.-T., Jehmlich, N. & Purswani, J. Actinobacterial Degradation of 2-Hydroxyisobutyric Acid Proceeds via Acetone and Formyl-CoA by Employing a Thiamine-Dependent Lyase Reaction. *Front. Microbiol.* **11**, 691 (2020).
37. Pfister, P., Zarzycki, J. & Erb, T. J. Structural Basis for a Cork-Up Mechanism of the Intra-Molecular Mesaconyl-CoA Transferase. *Biochemistry* **62**, 75–84 (2023).
38. Schulz-Mirbach, H. *et al.* New-to-nature CO2-dependent acetyl-CoA assimilation enabled by an engineered B12-dependent acyl-CoA mutase. *Nat Commun* **15**, 10235 (2024).
39. Roymoulik, I., Moon, N., Dunham, W. R., Ballou, D. P. & Marsh, E. N. G. Rearrangement of L-2-Hydroxyglutarate to L-*threo*-3-Methylmalate Catalyzed by Adenosylcobalamin-Dependent Glutamate Mutase. *Biochemistry* **39**, 10340–10346 (2000).
40. Wenk, S. *et al.* Evolution-assisted engineering of *E. coli* enables growth on formic acid at ambient CO2 via the Serine Threonine Cycle. *Metabolic Engineering* **88**, 14–24 (2025).
41. Scrutton, M. C., Griminger, P. & Wallace, J. C. Pyruvate Carboxylase. *Journal of Biological Chemistry* **247**, 3305–3313 (1972).
42. Scheffen, M. *et al.* A new-to-nature carboxylation module to improve natural and synthetic CO2 fixation. *Nature Catalysis* **4**, 105–115 (2021).

43. Rainaldi, V., Donati, S., D'Adamo, S. & Claassens, N. J. A recursive pathway for isoleucine biosynthesis arises from enzyme promiscuity. 2025.08.26.672309 Preprint at https://doi.org/10.1101/2025.08.26.672309 (2025).

44. Satanowski, A. *et al.* Awakening a latent carbon fixation cycle in Escherichia coli. *Nature Communications* **11**, 1–14 (2020).

45. Aoshima, M. & Igarashi, Y. A novel oxalosuccinate-forming enzyme involved in the reductive carboxylation of 2-oxoglutarate in Hydrogenobacter thermophilus TK-6. *Molecular Microbiology* **62**, 748–759 (2006).

46. Aoshima, M. & Igarashi, Y. Nondecarboxylating and Decarboxylating Isocitrate Dehydrogenases: Oxalosuccinate Reductase as an Ancestral Form of Isocitrate Dehydrogenase. *J Bacteriol* **190**, 2050–2055 (2008).

47. Buhrman, G. *et al.* Structure, Function, and Thermal Adaptation of the Biotin Carboxylase Domain Dimer from Hydrogenobacter thermophilus 2-Oxoglutarate Carboxylase. *Biochemistry* **60**, 324–345 (2021).

48. Marchal, D. G. *et al.* Machine Learning-Supported Enzyme Engineering toward Improved CO2-Fixation of Glycolyl-CoA Carboxylase. *ACS Synth. Biol.* **12**, 3521–3530 (2023).

49. Yang, X., Ma, Y., Yan, J., Zhao, G. & Zhang, Y. LATCH: a Linear Autocatalytic cycle Tailored for Carbon Harvesting. *Green Carbon* https://doi.org/10.1016/j.greenca.2025.10.003 (2025) doi:10.1016/j.greenca.2025.10.003.

50. Satanowski, A. *et al.* Design and implementation of aerobic and ambient CO2-reduction as an entry-point for enhanced carbon fixation. *Nat Commun* **16**, 3134 (2025).
51. Davidi, D. *et al.* Global characterization of in vivo enzyme catalytic rates and their correspondence to in vitro kcat measurements. *Proceedings of the National Academy of Sciences of the United States of America* **113**, 3401–3406 (2016).
52. Gale, N. & Beck, J. Evidence for the Calvin Cycle and Hexose Monophosphate Pathway in Thiobacillus ferrooxidans. https://journals.asm.org/doi/epdf/10.1128/jb.94.4.1052-1059.1967 (1967) doi:10.1128/jb.94.4.1052-1059.1967.
53. Dronsella, B. *et al. Engineered Synthetic One-Carbon Fixation Exceeds Yield of the Calvin Cycle*. http://biorxiv.org/lookup/doi/10.1101/2022.10.19.512895 (2022) doi:10.1101/2022.10.19.512895.
54. Bathellier, C., Tcherkez, G., Lorimer, G. H. & Farquhar, G. D. Rubisco is not really so bad. *Plant Cell Environ* **41**, 705–716 (2018).
55. Schulz-Mirbach, H., Dronsella, B. & Erb, T. J. Escherichia coli selection strains for growth-coupled metabolic engineering. *Trends in Biotechnology* **0**, (2025).
56. Gleizer, S. *et al.* Conversion of Escherichia coli to Generate All Biomass Carbon from CO2. *Cell* **179**, 1255-1263.e12 (2019).
57. Kim, S. *et al.* Growth of E. coli on formate and methanol via the reductive glycine pathway. *Nature Chemical Biology* **16**, 538–545 (2020).
58. Reiter, M. A. *et al.* A synthetic methylotrophic Escherichia coli as a chassis for bioproduction from methanol. *Nat Catal* **7**, 560–573 (2024).

59. Chen, F. Y. H., Jung, H. W., Tsuei, C. Y. & Liao, J. C. Converting Escherichia coli to a Synthetic Methylotroph Growing Solely on Methanol. *Cell* **182**, 933-946.e14 (2020).
60. Edwards, J. S., Ibarra, R. U. & Palsson, B. O. In silico predictions of Escherichia coli metabolic capabilities are consistent with experimental data. *Nat Biotechnol* **19**, 125–130 (2001).
61. Ebrahim, A., Lerman, J. A., Palsson, B. O. & Hyduke, D. R. COBRApy: COnstraints-Based Reconstruction and Analysis for Python. *BMC Systems Biology* **7**, 74 (2013).
62. Bizouarn, T., Van Boxel, G. I., Bhakta, T. & Jackson, J. B. Nucleotide binding affinities of the intact proton-translocating transhydrogenase from Escherichia coli. *Biochimica et Biophysica Acta - Bioenergetics* **1708**, 404–410 (2005).
63. Elad Noor / ged-cycle · GitLab. *GitLab* https://gitlab.com/elad.noor/ged-cycle (2024).
64. Chang, A. *et al.* BRENDA, the ELIXIR core data resource in 2021: new developments and updates. *Nucleic Acids Res* **49**, D498–D508 (2021).

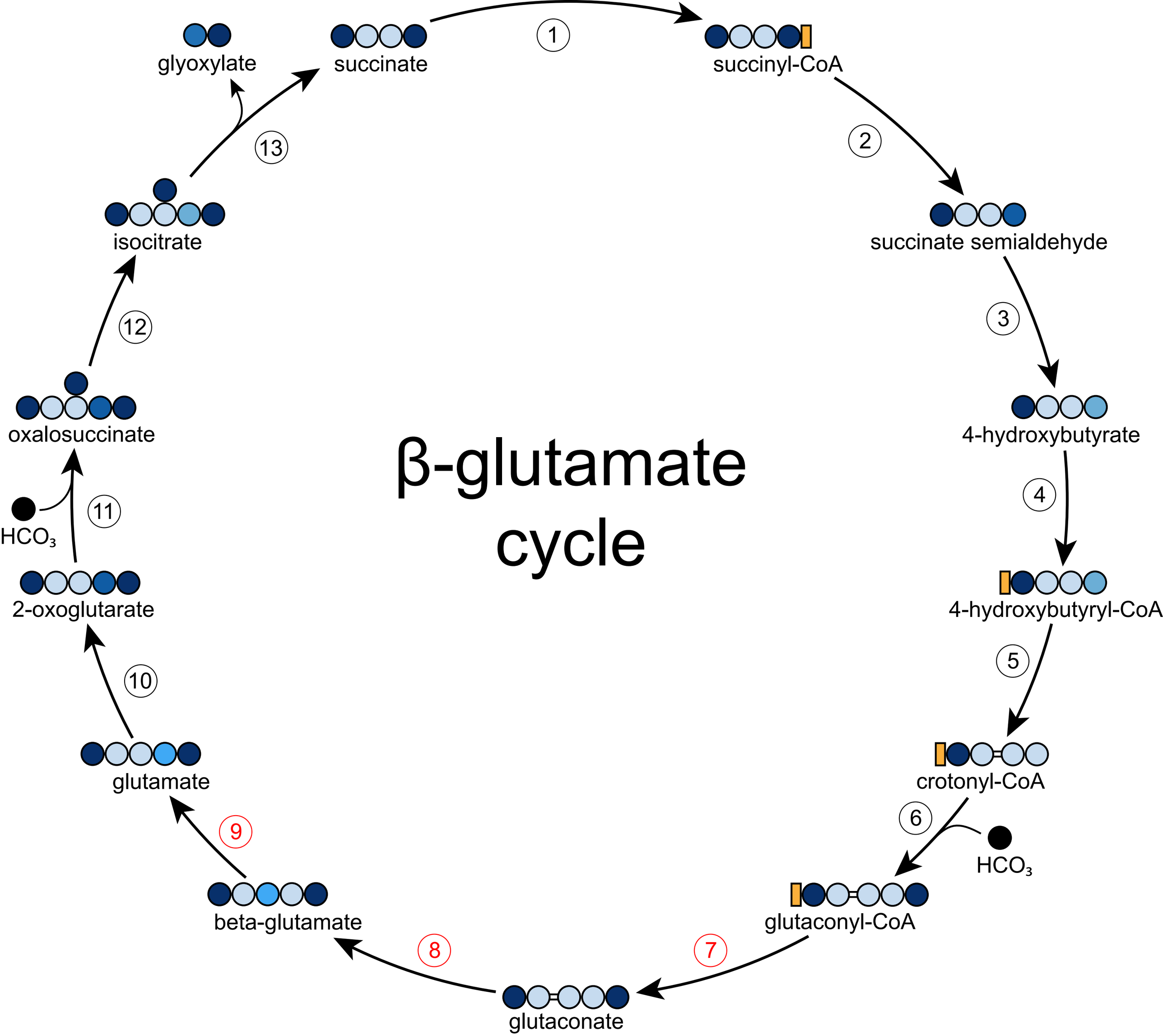
β-glutamate cycle
succinate
succinyl-CoA
succinate semialdehyde
4-hydroxybutyrate
4-hydroxybutyryl-CoA
crotonyl-CoA
HCO_3
glutaconyl-CoA
glutaconate
beta-glutamate
glutamate
2-oxoglutarate
HCO_3
oxalosuccinate
isocitrate
glyoxylate
1
2
3
4
5
6
7
8
9
10
11
12
13

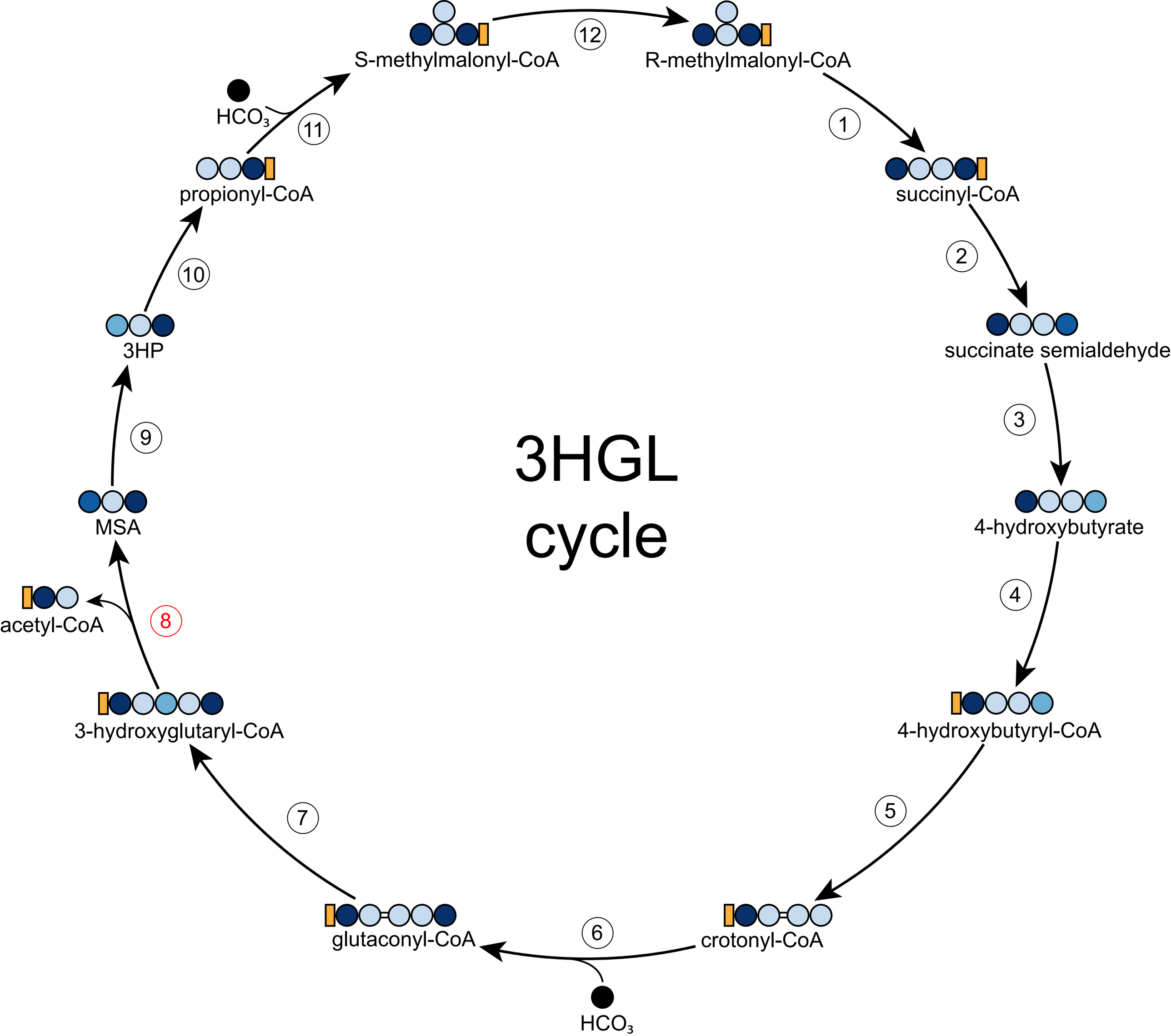
3HGL
cycle
S-methylmalonyl-CoA
R-methylmalonyl-CoA
12
1
succinyl-CoA
2
succinate semialdehyde
3
4-hydroxybutyrate
4
4-hydroxybutyryl-CoA
5
crotonyl-CoA
6
HCO3
glutaconyl-CoA
7
3-hydroxyglutaryl-CoA
8
acetyl-CoA
MSA
9
3HP
10
propionyl-CoA
11
HCO3

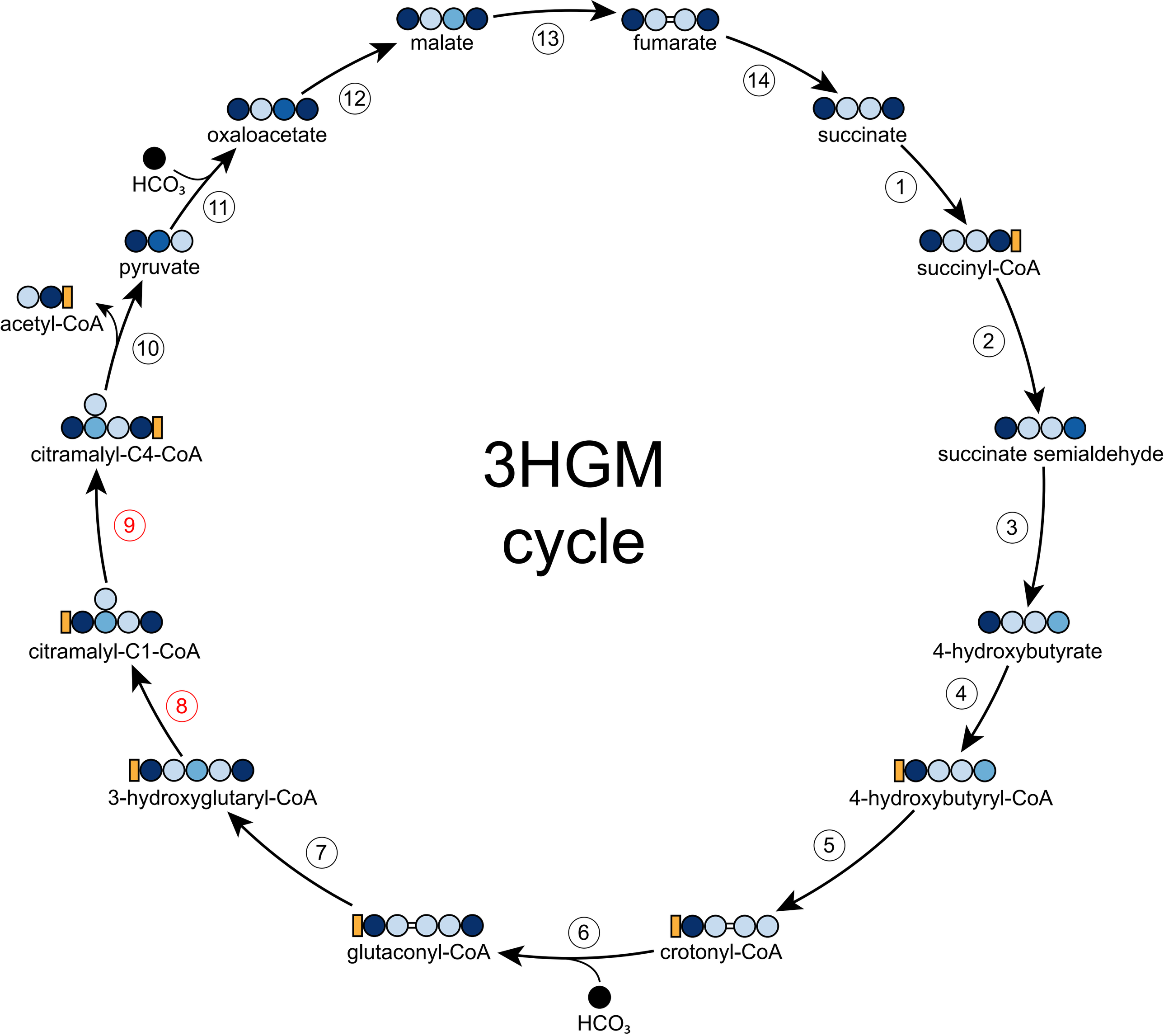
3HGM
cycle
malate
fumarate
oxaloacetate
succinate
pyruvate
succinyl-CoA
acetyl-CoA
succinate semialdehyde
citramalyl-C4-CoA
4-hydroxybutyrate
citramalyl-C1-CoA
4-hydroxybutyryl-CoA
3-hydroxyglutaryl-CoA
glutaconyl-CoA
crotonyl-CoA
HCO3
HCO3
1
2
3
4
5
6
7
8
9
10
11
12
13
14

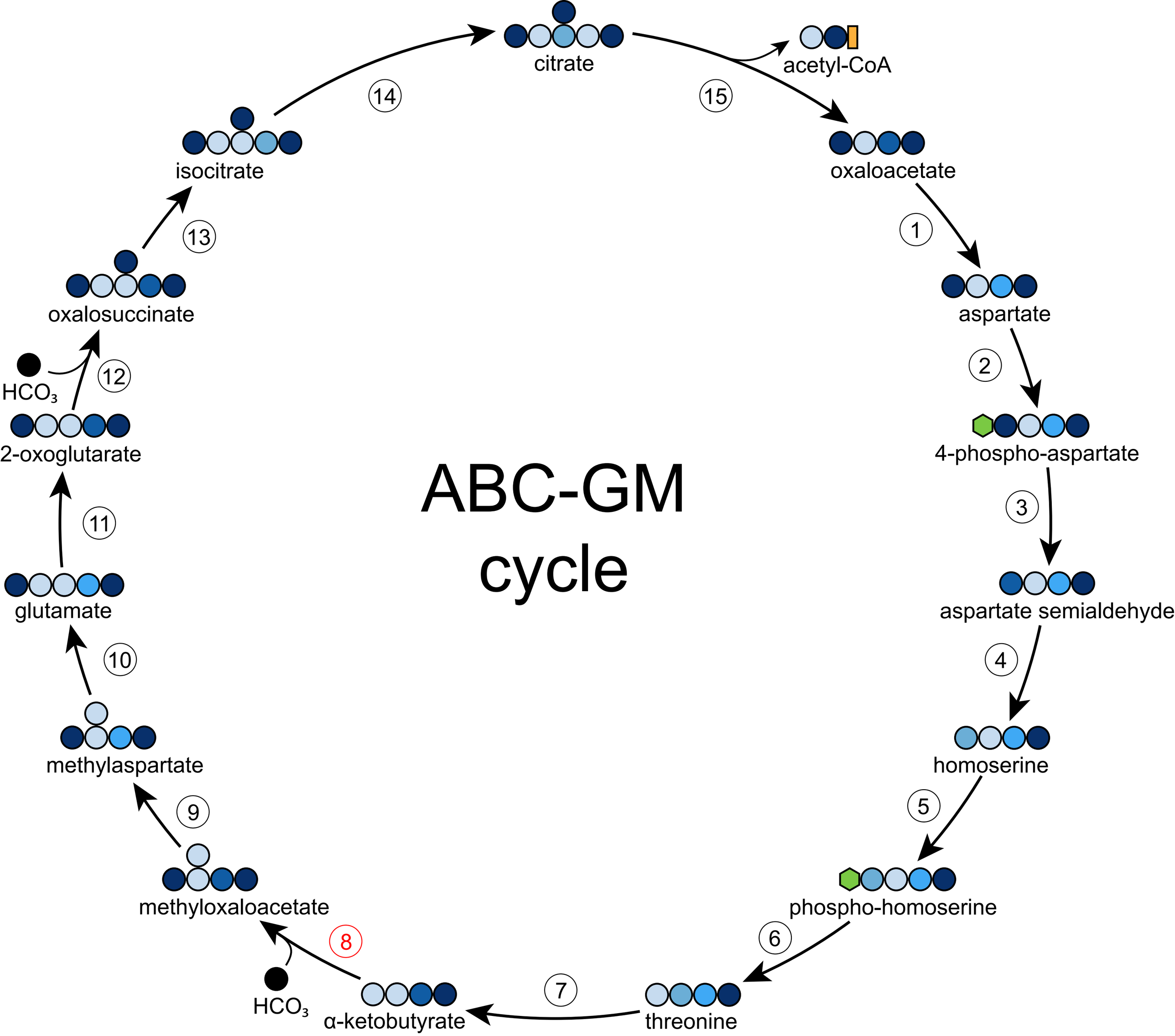
ABC-GM
cycle
citrate
acetyl-CoA
oxaloacetate
aspartate
4-phospho-aspartate
aspartate semialdehyde
homoserine
phospho-homoserine
threonine
α-ketobutyrate
methyloxaloacetate
methylaspartate
glutamate
2-oxoglutarate
oxalosuccinate
isocitrate
HCO_3
HCO_3
1
2
3
4
5
6
7
8
9
10
11
12
13
14
15

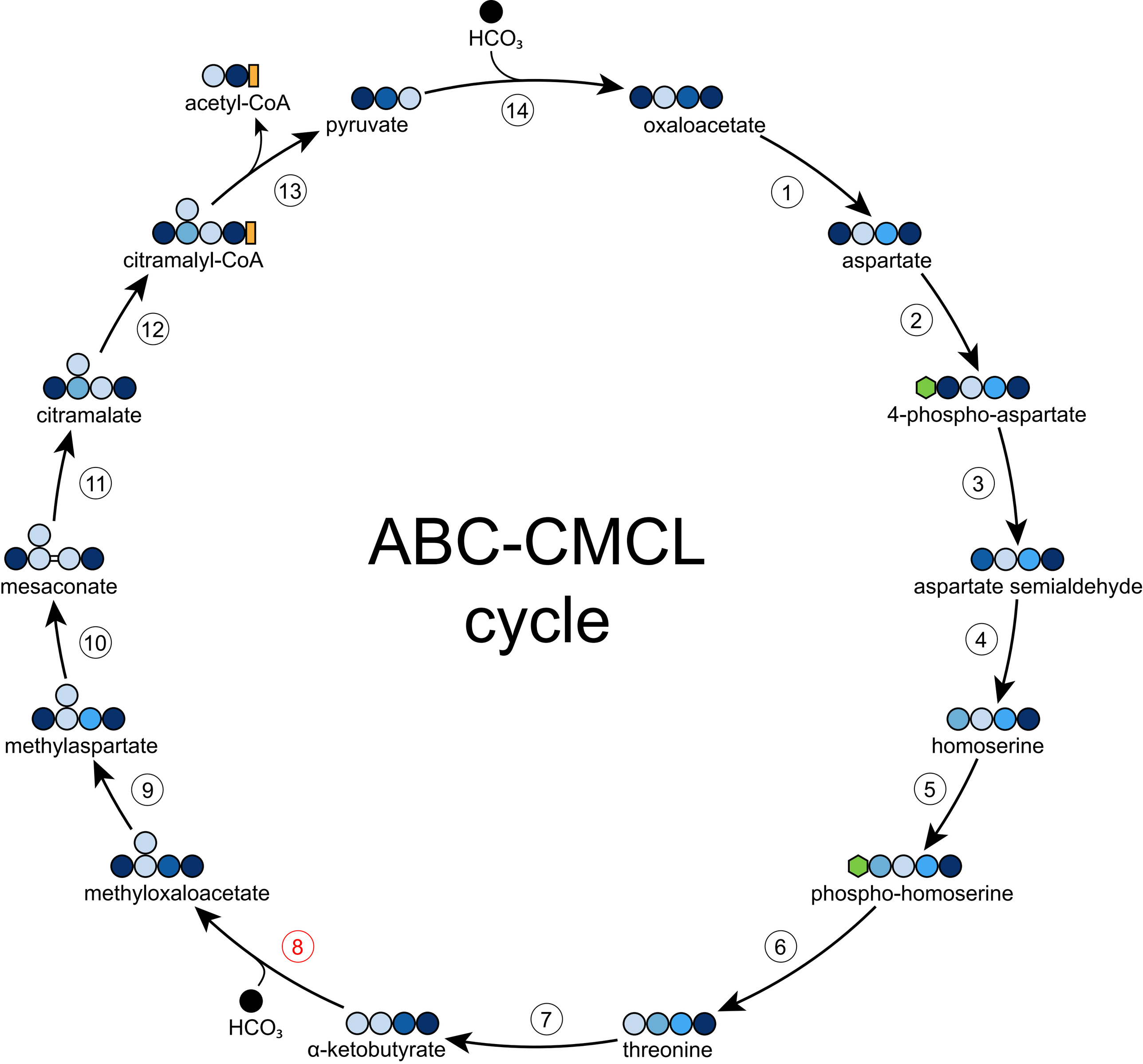
ABC-CMCL
cycle
HCO3
14
pyruvate
oxaloacetate
acetyl-CoA
13
citramalyl-CoA
1
aspartate
2
4-phospho-aspartate
12
citramalate
3
11
mesaconate
aspartate semialdehyde
10
4
methylaspartate
homoserine
9
5
methyloxaloacetate
phospho-homoserine
8
6
HCO3
7
α-ketobutyrate
threonine

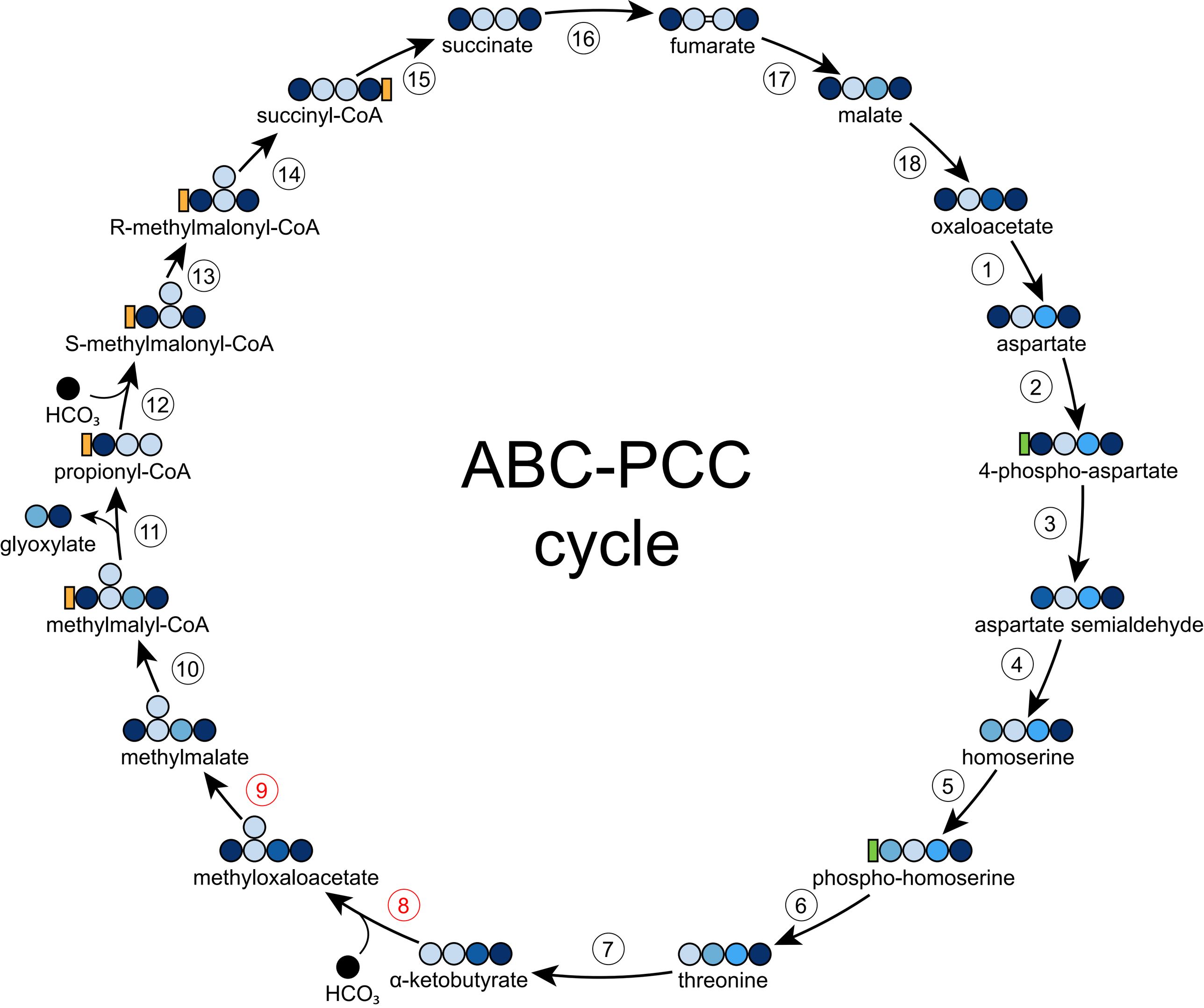
ABC-PCC
cycle
succinate
fumarate
malate
oxaloacetate
aspartate
4-phospho-aspartate
aspartate semialdehyde
homoserine
phospho-homoserine
threonine
α-ketobutyrate
HCO3
methyloxaloacetate
methylmalate
methylmalyl-CoA
glyoxylate
propionyl-CoA
HCO3
S-methylmalonyl-CoA
R-methylmalonyl-CoA
succinyl-CoA
1
2
3
4
5
6
7
8
9
10
11
12
13
14
15
16
17
18

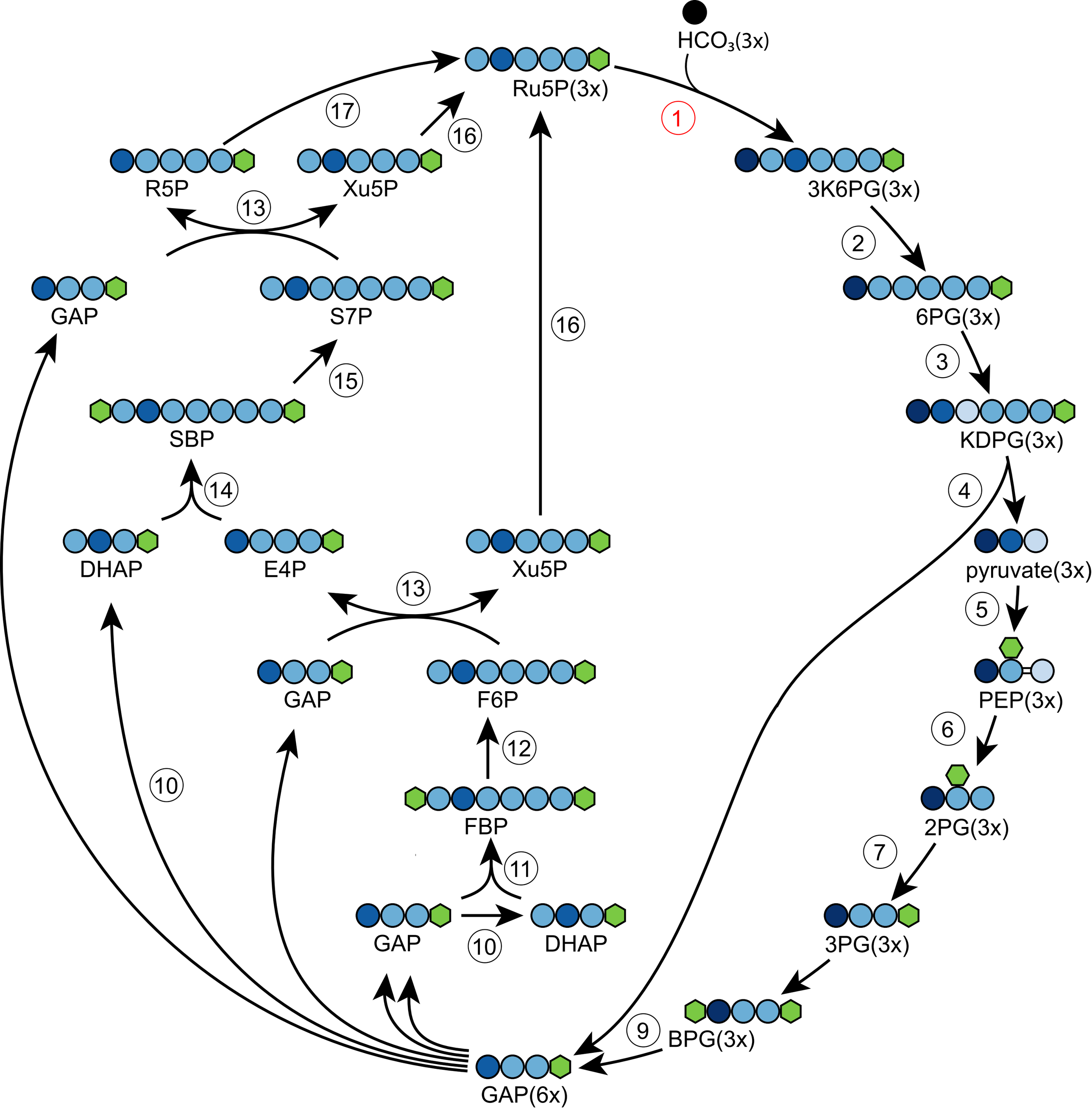
HCO3(3x)
Ru5P(3x)
1
3K6PG(3x)
2
6PG(3x)
3
KDPG(3x)
4
pyruvate(3x)
5
PEP(3x)
6
2PG(3x)
7
3PG(3x)
BPG(3x)
9
GAP(6x)
10
GAP
DHAP
11
FBP
12
F6P
GAP
13
Xu5P
E4P
DHAP
14
SBP
15
S7P
GAP
16
Xu5P
R5P
13
16
17

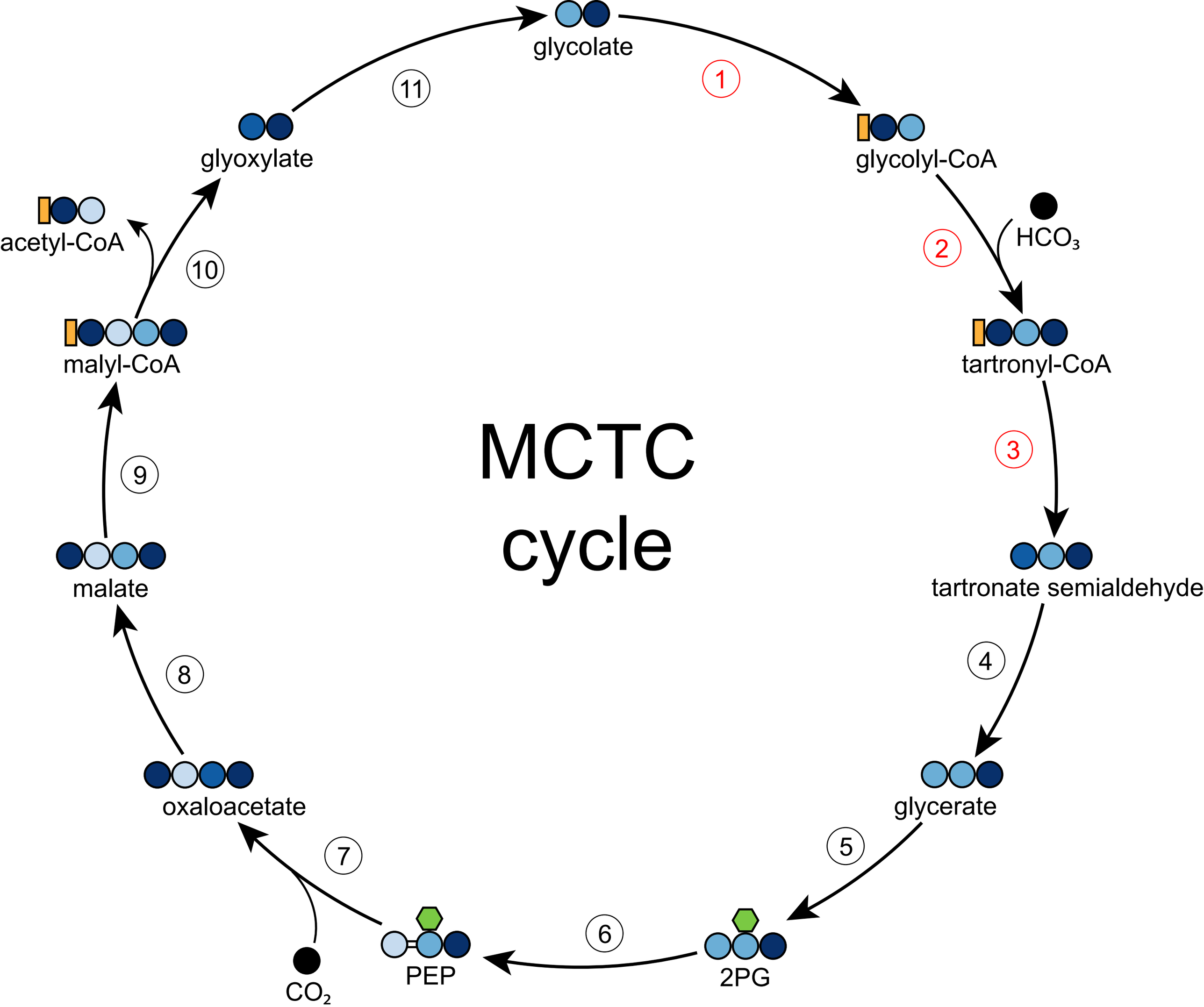
MCTC
cycle
glycolate
glycolyl-CoA
HCO_3
tartronyl-CoA
tartronate semialdehyde
glycerate
2PG
PEP
CO_2
oxaloacetate
malate
malyl-CoA
acetyl-CoA
glyoxylate
1
2
3
4
5
6
7
8
9
10
11

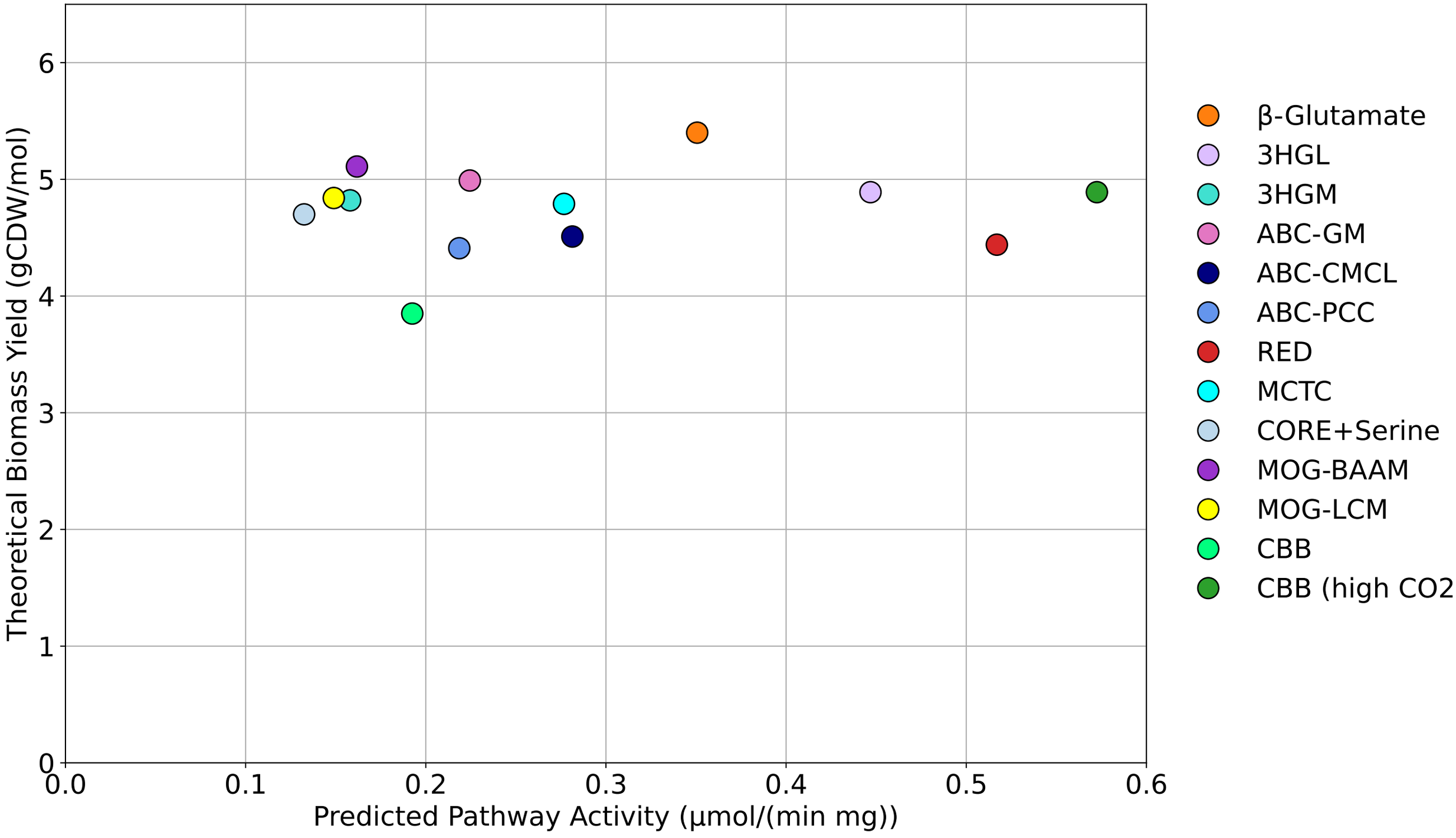
Theoretical Biomass Yield (gCDW/mol)
Predicted Pathway Activity (μmol/(min mg))
0
1
2
3
4
5
6
0.0
0.1
0.2
0.3
0.4
0.5
0.6
β-Glutamate
3HGL
3HGM
ABC-GM
ABC-CMCL
ABC-PCC
RED
MCTC
CORE+Serine
MOG-BAAM
MOG-LCM
CBB
CBB (high CO2)

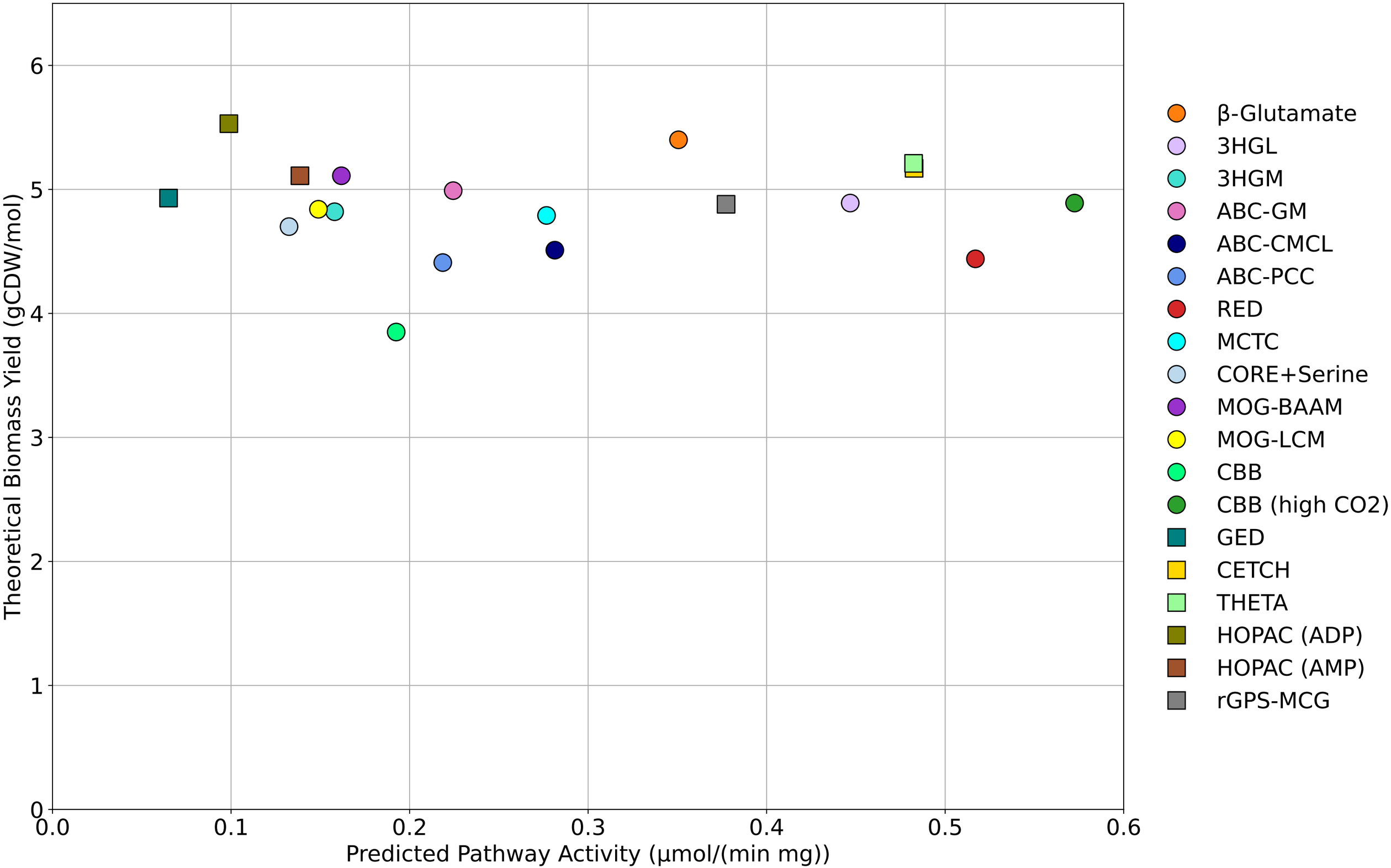
Theoretical Biomass Yield (gCDW/mol)
Predicted Pathway Activity (µmol/(min mg))
0
1
2
3
4
5
6
0.0
0.1
0.2
0.3
0.4
0.5
0.6
β-Glutamate
3HGL
3HGM
ABC-GM
ABC-CMCL
ABC-PCC
RED
MCTC
CORE+Serine
MOG-BAAM
MOG-LCM
CBB
CBB (high CO2)
GED
CETCH
THETA
HOPAC (ADP)
HOPAC (AMP)
rGPS-MCG